FNP

JOURNAL OF FOOD PROCESS ENGINEERING

D.R. HELDMAN
and
R.P. SINGH
COEDITORS

FOOD & NUTRITION PRESS, INC.

VOLUME 10, NUMBER 4

QUARTERLY

JOURNAL OF FOOD PROCESS ENGINEERING

All articles for publication and inquiries regarding publications should be sent to either DR. D.R. HELDMAN, COEDITOR, *Journal of Food Process Engineering,* National Food Processors Association, 1401 New York Ave., N.W., Washington, D.C. 20005 USA; or DR. R.P. SINGH, COEDITOR, *Journal of Food Process Engineering,* University of California, Davis, Department of Agricultural Engineering, Davis, CA 95616 USA.

All subscriptions and inquiries regarding subscription should be sent to Food & Nutrition Press, Inc., 6527 Main Street, P.O. Box 374, Trumbull, Connecticut 06611 USA.

One volume of four issues will be published annually. The price for Volume 10 is $80.00 which includes postage to U.S., Canada, and Mexico. Subscriptions to other countries are $94.00 per year via surface mail, and $102.00 per year via airmail.

Subscriptions for individuals for their own personal use are $60.00 for Volume 10 which includes postage to U.S., Canada, and Mexico. Personal subscriptions to other countries are $74.00 per year via surface mail, and $82.00 per year via airmail. Subscriptions for individuals should be sent to the publisher and marked for personal use.

The *Journal of Food Process Engineering* (ISSN 0145-8876) is published quarterly (March, June, September and December) by Food & Nutrition Press, Inc.—Office of Publication is 6527 Main Street, P.O. Box 374, Trumbull, Connecticut 06611 USA. (Current issue is March 1989).

Second class postage paid at Bridgeport, CT 06602.

POSTMASTER: Send address changes to Food & Nutrition Press, Inc., 6527 Main Street, P.O. Box 374, Trumbull, CT 06611.

JOURNAL OF FOOD PROCESS ENGINEERING

JOURNAL OF FOOD PROCESS ENGINEERING

Journal of
FOOD PROCESS ENGINEERING

VOLUME 10
NUMBER 4

Coeditors: D.R. HELDMAN
R.P. SINGH

FOOD & NUTRITION PRESS, INC.
TRUMBULL, CONNECTICUT 06611 USA

ISSN 0145-8876

Printed in the United States of America

CONTENTS

CONDUCTION HEATING OF HIGH MOISTURE ROUGH RICE
I. THERMAL INACTIVATION OF FUNGI

V. G. REYES, JR. and V. K. JINDAL

Division of Agricultural and Food Engineering
Asian Institute of Technology
P. O. Box 2754
Bangkok, Thailand 10501

Accepted for Publication June 27, 1988

ABSTRACT

Conduction heating of high moisture rough rice was evaluated as a means of arresting fungal growth using an experimental batch-type rotary heating unit. The heat treatments significantly reduced fungal activity in rough rice as measured by dilution plating and carbon dioxide production. The effectiveness of heat treatments depended upon the exposure time and heating surface temperature. Exposure times for isothermal heating of rough rice were determined for inactivating the fungi to specified mortality levels based on the heating surface temperature. Subsequently, a general procedure which accounted for the heating lags was developed for estimating the heat dosages based on the time-temperature history of the bulk grain during conduction heating in any given equipment.

INTRODUCTION

The main factor contributing to the spoilage of high moisture rough rice is the development of fungi, spores of which are already present in the field at the time of harvest (Schroeder and Sorenson 1961; Schroeder 1967; Mendoza *et al.* 1981; Ilag 1982; Quitco 1982). Therefore, drying of rough rice to moisture levels too low for microorganisms to grow is the most effective and widely used method of preserving grain quality. In Southeast Asia, the advent of high-yielding varieties and second season crops that mature during the rainy season has resulted in a much greater load on the already insufficient drying facilities. Consequently, some of the rough rice can not be dried immediately during the peak harvesting period. It must be temporarily stored at high moisture contents and it may deteriorate due to rapid fungal growth.

Journal of Food Process Engineering 10 (1989) 231-248.

Several methods which have been attempted in the past to extend the safe storage period of high moisture rough rice prior to drying include the use of chemical preservatives, aeration, controlled atmosphere storage, and low temperature storage (Sauer and Burroughs 1974; Calderwood and Schroeder 1975; Schroeder and Sorenson 1961; Calderwood 1966; de Padua 1965; Hyde 1969; Iwasaki and Tani 1967; Kreyger 1963). These methods have been used with limited success mainly because of high costs and the development of undesirable taste and odor in the stored rice.

The inactivation of microorganisms by the application of heat is common in food processing industry but it has not been applied to preserve the quality of high moisture grains. Though maximum temperatures for fungal growth in grains have been reported to be in the range of 50 to 55°C, the maximum exposure times which the fungi can tolerate are not known (Ayerst 1969; Christensen and Kaufmann 1974). Conduction heating of high moisture rough rice for inactivating the fungi could prove to be an innovative and practical approach for temporarily holding wet grain prior to final drying. However, evaluation of this approach must include detailed investigations of the time-temperature history of the grain during conduction heating, the operational characteristics of the heat application system and the changes in grain quality due to heating. This approach could be practical because conduction heating equipment generally require less capital investment and energy, and such equipment are easy to fabricate (Chancellor 1968; Root and Cook 1980).

In this study, the thermal inactivation of fungi present in freshly harvested high moisture rough rice was investigated using a rotary conduction heating unit. Time-temperature requirements to achieve the desired levels of fungal mortality are presented using the bulk grain temperature as a reference.

MATERIALS AND METHODS

Preparation of Rough Rice Samples

Rough rice used for this study was a medium grain variety (RD-23) which was harvested between November 1985 to February 1986. Rice was harvested by sickle and then fed through a stationary thresher. Immediately after harvesting, the moisture content of the rough rice ranged from 22 to 24% wet basis (w.b.). To ensure a uniform initial moisture of samples, moisture was adjusted to about 26% (w.b.) by addition of water. Rough rice samples were placed in plastic bags and kept in cold storage (5°C) for about 24 h to allow equilibration. Afterwards, the samples were temporarily stored in a freezer at −15°C to minimize fungal growth and quality changes until the test time. Prior to heating tests, the frozen sample was thawed at room temperature (about 30°C) over a period of about 8 h while in plastic bags.

Experimental Batch-Type Rotary Conduction Heating Unit

A rotary batch-type conduction heating unit was designed, fabricated and used for heating experiments (Fig. 1). The heating unit mainly consisted of a rotary cylinder, 0.35 m in diameter and 0.85 m long, with six equidistant straight axial flights extending 4 cm from the inside surface. A heavy duty ball bearing mounted on the steel frame supported the cylinder from one side during its rotation. The other end of the cylinder served as the inlet and outlet for rice samples and had a removable perforated cover. Samples were discharged by removing the cover and lifting the rear side of the unit. Four 1-kW electrical resistance heaters were placed beneath the rotary cylinder to supply the required heat. The heaters and rotary cylinder were encased in an outer cylinder and insulated using a 6 cm thick wool fibre packing. The temperature of the cylinder surface could be raised to 300°C and maintained within ± 5°C by a temperature controller. The cylinder rotation speed could be adjusted from 10 to 40 rpm by a variable speed 1-kW electric motor.

Heating of Rough Rice Samples

Rough rice samples were heated in batches of 3 kg each using the experimental rotary unit. Four heating surface temperatures of 75, 100, 150, 200°C and exposure times ranging from 3 to 40 min were used. The cylinder rotation speed was fixed at 30 rpm to ensure faster heating rates. The time-temperature profiles of the bulk grain were monitored during heating and cooling processes. The temperature of the bulk grain was measured with a thermocouple sensor by transferring the heated grain sample into a vacuum flask and allowing it to attain a steady state value. This procedure enabled the monitoring of the time-temperature profiles of the bulk grain during the heating and as well as cooling processes.

Heat-treated rough rice samples were immediately transferred to the aluminum trays where they were spread in 5 cm layers, completely covered with aluminum foil, and cooled to room temperature in a chamber maintained at −15°C. A small portion of the heated sample was placed into a vacuum flask for grain temperature measurement. Cooling of rice samples in a fully enclosed container was necessary to prevent any contamination prior to microbiological testing. This method resulted in a cooling of rice samples at the rate of approximately 2°C/min.

Immediately after cooling, the sample was divided into two subsamples, one for measurement of fungal count and another for carbon dioxide production.

Measurement of Fungal Activity

The number and proportion of fungi present in the rough rice samples were determined by dilution plating assay as described by Flannigan (1977). Malt-

1. Rotary heating chamber
2. Straight flights
3. Inlet / outlet
4. Removable cover
5. Fixed outer casing
6. Electric heater
7. Variable speed motor
8. Paddy outlet guide
9. Chain drive
10. Handle
11. Temperature controller

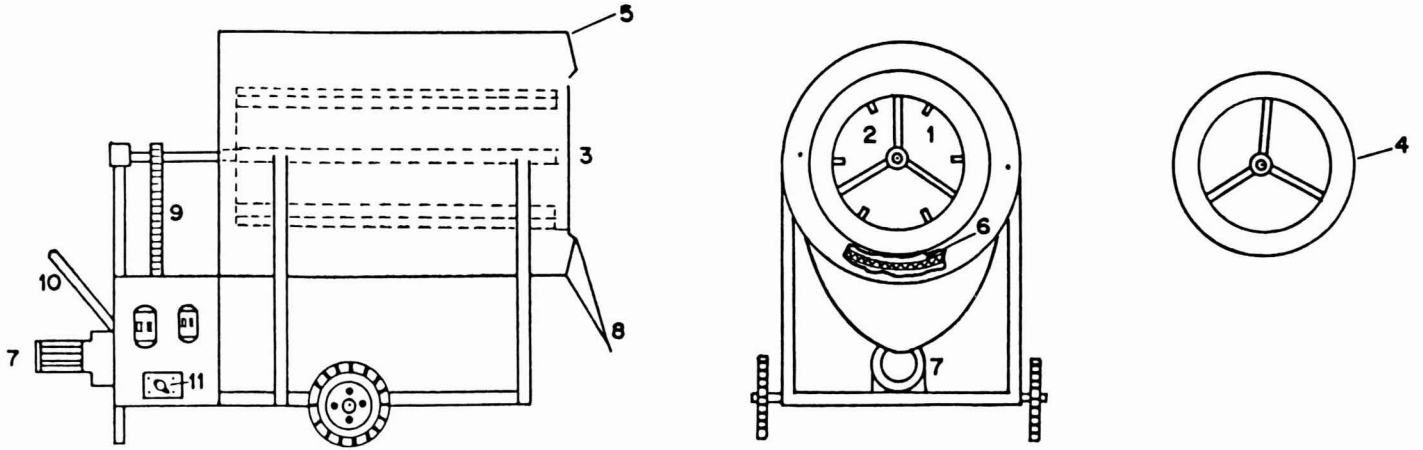

FIG. 1 SCHEMATIC DIAGRAM OF THE BATCH-TYPE ROTARY CONDUCTION HEATING UNIT

salt and potato dextrose agar were used to detect storage and field fungi, respectively. Dilutions were made by blending 50 g of grain in 500 mL of 0.12% sterile agar in water for 2 min. Successive dilutions were made by transferring 10 mL of the suspension medium to 90 mL of 0.12% agar in water. One-mL and 0.2 mL of appropriate dilutions were cultured in sterilized dishes containing malt-salt (6% NaCl) and potato dextrose agar media, respectively. The number of fungal colonies on the dilution plates were counted after 5 to 10 days of incubation at 25–30°C.

The production of carbon dioxide by rough rice samples was also measured by chemical absorption system similar to Steele *et al.* (1969) and Fernandez *et al.* (1985). The system which uses a sample size of 1 kg was operated at room temperature (30°C) for about 24 h per tests. Other details of fungal activity and carbon dioxide measurements are given by Reyes (1986).

The effectiveness of heat treatments for inactivating the fungi present in freshly harvested rough rice was described in terms of a fungal load ratio (FLR) and fungal mortality level (FML) defined as,

$$FLR = FC_i / FC_o \quad (1)$$

$$FML = (1 - FLR) \times 100 \quad (2)$$

Where FC_i = fungal count in heat-treated rough rice sample, colonies/g
FC_o = fungal count in unheated rough rice sample (control), colonies/g

RESULTS AND DISCUSSION

Fungi Present in Freshly Harvested Rough Rice

Table 1 shows the various fungi detected in freshly harvested high moisture rough rice along with their respective proportions. The results presented are the average of three replications. The coefficient of variation for all tests ranged from 10–30%. The fungal counts ranged approximately from 1,300 to 5,500 colonies/g. The apparent large variability in the fungal counts was perhaps due to the changes during the holding periods, sampling process, and the test method itself. In general, *Penicillium* species, *Helminthosporium,* and *Aspergillus flavus* made up the bulk of the count in all of the samples. These fungi are usually considered to cause declines in grain quality during temporary storage at high moisture content (Tatsumo 1963; Fazli and Schroeder 1966a, b; Schroeder 1967; Christensen and Kaufmann 1974; Quitco 1982). Also present were species of

TABLE 1.
FUNGI PRESENT IN FRESHLY HARVESTED PADDY OF VARIETY RD-23

Fungi	Test Number							
	1	2	3	4	5	6	7	8
Helminthosporium	600	600	600	25	500	0	250	0
Rhizopus	100	20	70	1200	0	600	100	0
Mucor	100	50	100	500	0	0	0	0
Penicillium spp.	250	590	900	3170	2500	1200	1200	400
Aspergillus flavus	65	40	130	500	500	1500	50	1200
Aspergillus niger	50	0	0	0	500	1300	50	300
Aspergillus terreus and A. versicolor	0	0	0	100	500	0	0	0
Total fungal count (colonies/g)	1350	1300	1800	5500	4500	5200	1650	2000

Rhizopus, Mucor, Aspergillus terreus and *Aspergillus versicolor* in relatively smaller proportions.

Table 2 presents the proportion of fungal species surviving in rough rice following the heat treatment corresponding to approximately 90% fungal mortality level. It was obvious that the storage fungi such as *Aspergillus flavus, Aspergillus niger* and *Penicillium* species were most heat resistant. However, most of the field fungi were reduced to a very low level after the heat treatment.

Relationship Between Fungal Count and Carbon Dioxide Production

There appeared to be a direct relationship between the respiration rate of the rough rice samples in terms of carbon dioxide production and the total fungal count determined by the dilution plating. Heat treatment of rough rice samples

TABLE 2.
SURVIVAL OF VARIOUS FUNGI IN FRESHLY HARVESTED ROUGH RICE FOLLOWING THE HEAT TREATMENT CORRESPONDING TO ABOUT 90% MORTALITY LEVEL

Fungi	Percent survival	Standard deviation
Helminthosporium spp.	0.2	0.06
Rhizopus spp.	0.3	0.07
Mucor spp.	0.2	0.02
Penicillium spp.	5.2	1.04
Aspergillus flavus	2.1	0.60
Aspergillus niger	1.6	0.48
Aspergillus terreus	0.4	0.10

resulted in a marked reduction in the carbon dioxide production perhaps due to the destruction of fungi cells and reduced grain viability.

The fungal count of rough rice samples was found to be highly correlated with carbon dioxide production as shown by the following relationship:

$$Y = a + b\,X + c\,X^2 + d\,X^3 \quad (3)$$

Where Y = log of fungal count in colonies/g
X = log of carbon dioxide production in mg/kg-day
a,b,c,d = regression coefficients

The regression coefficients of Eq. 3 fitted into the experimental data are given in Table 3. These results were found to be in agreement with an earlier study made by Lin (1985) which covered a wider range of fungal activity (Fig. 2). Therefore, a third degree polynomial (Eq. 3) adequately described the combined data shown in Fig. 2. This suggests that carbon dioxide production could be used as an alternative method of estimating fungal activity. Since the experimental procedures for carbon dioxide measurement are simpler than dilution plating assays, monitoring of fungal activity indirectly would be more practical especially with a large number of rough rice samples.

Time-Temperature History of Rough Rice Samples During Conduction Heating

The bulk grain temperature of rough rice samples during conduction heating was adequately described by the following relationships based on regression analysis:

$$T_{gi} = T_s - (T_{go} - T_s)\ \exp\left(-c_1\ t^{0.28}\right) \quad (4)$$

TABLE 3.
REGRESSION COEFFICIENTS OF THE RELATIONSHIP BETWEEN FUNGAL COUNT AND CARBON DIOXIDE PRODUCTION (EQ. 3)

Reference	a	b	c	d	R^2	SEE
Present study	1.5261	0.8520	-	-	0.810	0.30
Lin (1985)	2.5341	-1.0209	0.8176	-0.0405	0.896	0.79
Present study and Lin (1985)	2.4588	-0.7674	0.5950	-	0.860	0.77

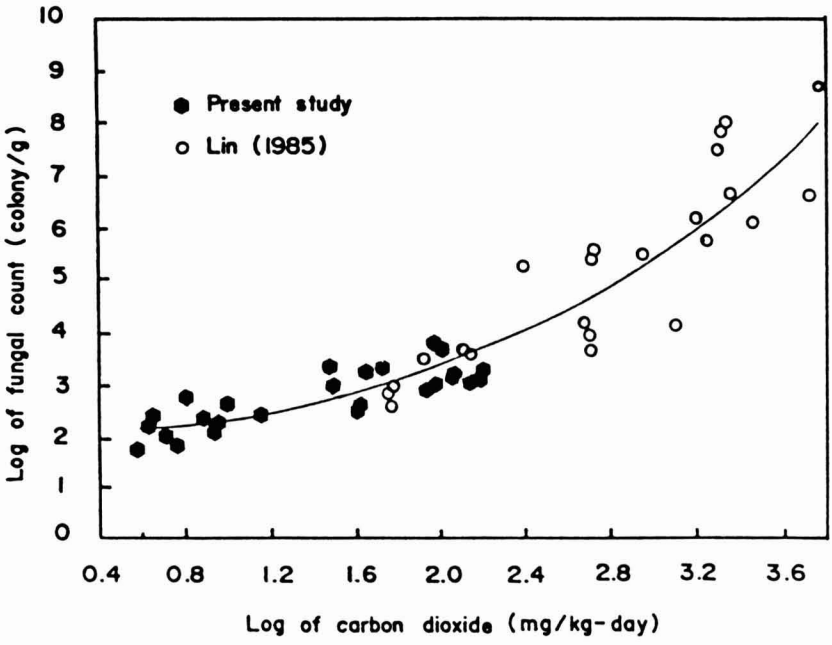

FIG. 2 FUNGAL COUNT AS A FUNCTION OF CARBON DIOXIDE PRODUCTION IN ROUGH RICE SAMPLES

$$c_1 = 0.4353 - 0.0006618\ T_s - 0.0001105\ (M_o)^2 + 0.0003607\ N \quad (5)$$

($R^2 = 0.90$; SEE = 0.014)

Where T_{gi} = bulk grain temperature during heating, °C
T_s = heating surface temperature, °C
T_{go} = initial grain temperature, °C
t = heating time, min
c_1 = regression coefficient
N = cylinder rotation speed, revolutions/min
M_o = initial moisture content of rough rice, % w.b.

A comparison of experimental data points and estimated time-temperature history of rough rice samples for various heating surface temperatures is shown in Fig. 3. It was also observed that the moisture content of rough rice samples

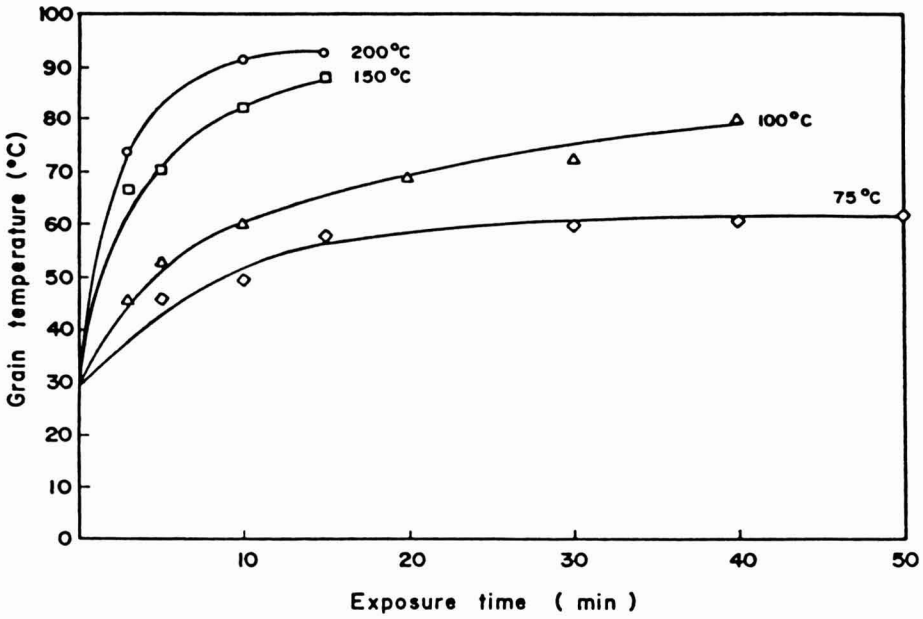

FIG. 3 GRAIN TEMPERATURE AS A FUNCTION OF EXPOSURE DURATION FOR VARIOUS HEATING SURFACE TEMPERATURES

was markedly reduced due to conduction heating, especially for higher heating surface temperatures (Fig. 4).

Thermal Inactivation of Fungi in High Moisture Rice

Figure 5 presents the relationship between fungal load ratio and exposure time during conduction heating of high moisture rice samples for various heating surface temperatures. A distinct reduction in fungal activity was obvious in all heating experiments. As expected, higher heating surface temperatures resulted in shorter exposure durations in reducing the fungal load to a specific level. Reduced fungal activity accompanied by partial drying of high moisture rice as seen in Fig. 4 could potentially allow the grain to be temporarily held without significant deterioration.

The plots of fungal load ratio versus exposure time for various heating surface temperatures (Fig. 5) enabled the computation of actual heating times or F_s-values corresponding to arbitrarily selected fungal mortality levels (Ball and Olson 1957; Bradshaw *et al.* 1982; Holdsworth 1985). The exposure times (F_s-values) needed to achieve 75, 90 and 95% fungal mortality levels are presented

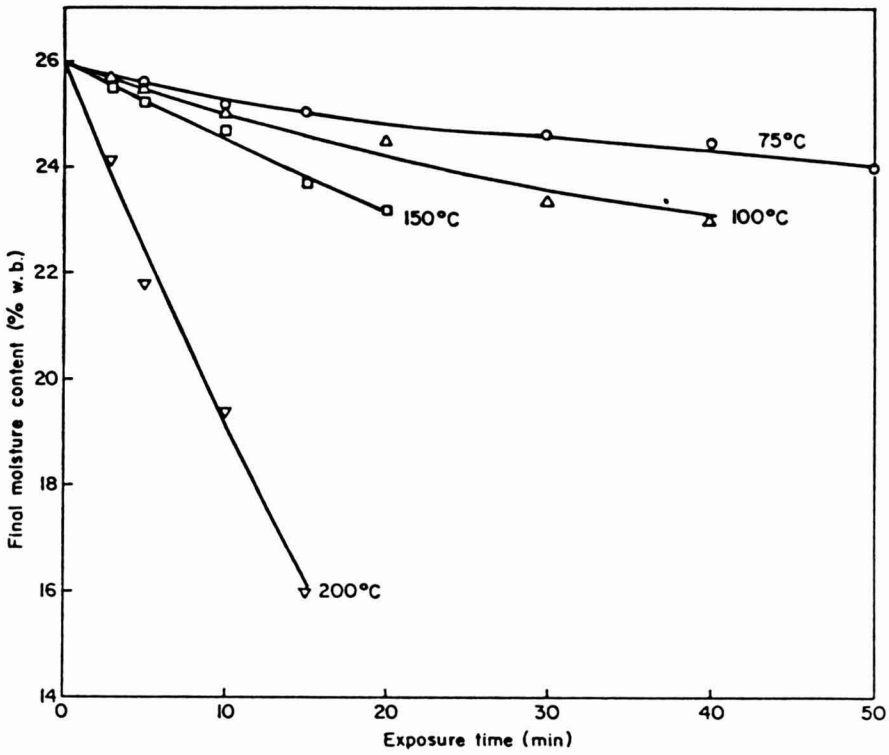

FIG. 4 FINAL MOISTURE CONTENT AS A FUNCTION OF EXPOSURE DURATION FOR VARIOUS HEAT TREATMENT COMBINATIONS

as a function of heating surface temperature in Fig. 6. The relationships of Fig. 6 can be expressed by the following equation which is based on regression analysis:

$$\text{Log } F_s = a_0 + a_1 T_s \tag{6}$$

Where F_s = actual heating time to achieve a specific fungal mortality level, min
T_s = heating surface temperature, °C
a_0, a_1 = regression coefficients

The determination of z_s-values shown in Table 4 describe the temperature dependence of F_s-values on the inverse of the slope of the thermal death time curve (Fig. 5) or $1/a_1$, when using Eq. 6. Finally, the heating time to achieve a desired

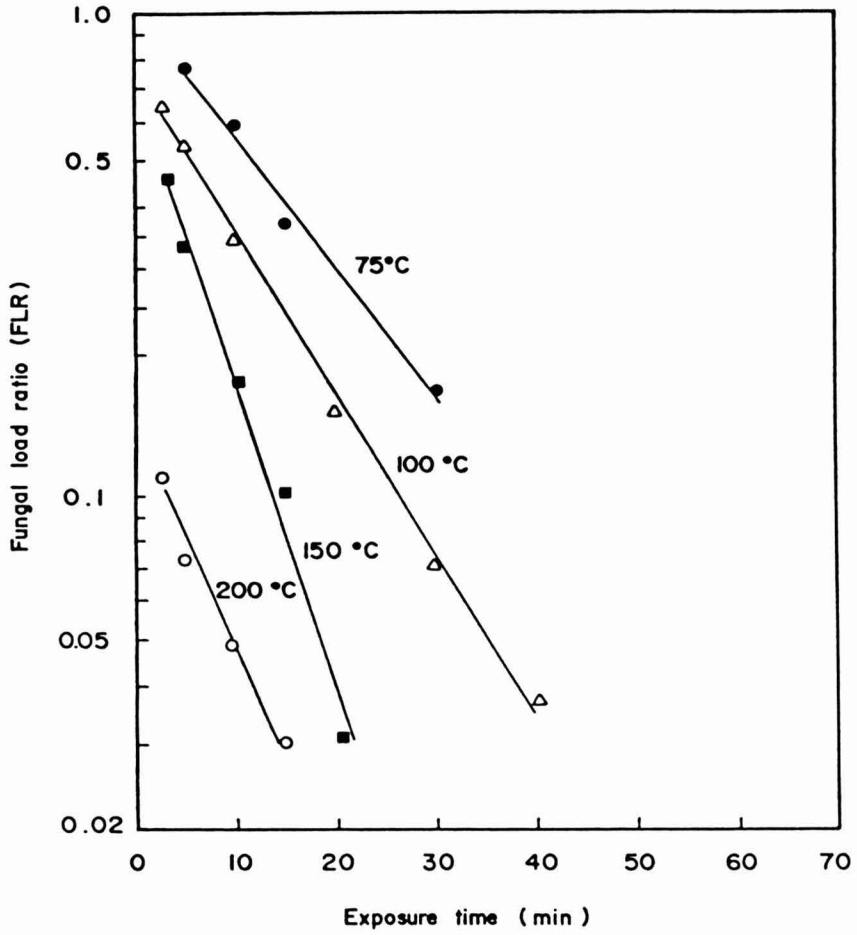

FIG. 5 FUNGAL LOAD RATIO AS A FUNCTION OF EXPOSURE DURATION FOR VARIOUS HEATING SURFACE TEMPERATURES

level of fungal mortality could be estimated by the following relationship (Bigelow *et al.* 1920):

$$Fs = Fo \; 10^{[\,Tref - Ts\,]/zs} \tag{7}$$

Where F_0 = exposure time at a reference temperature, min
T_{ref} = reference heating surface temperature, °C
z_s = z-value based on heating surface temperature, °C

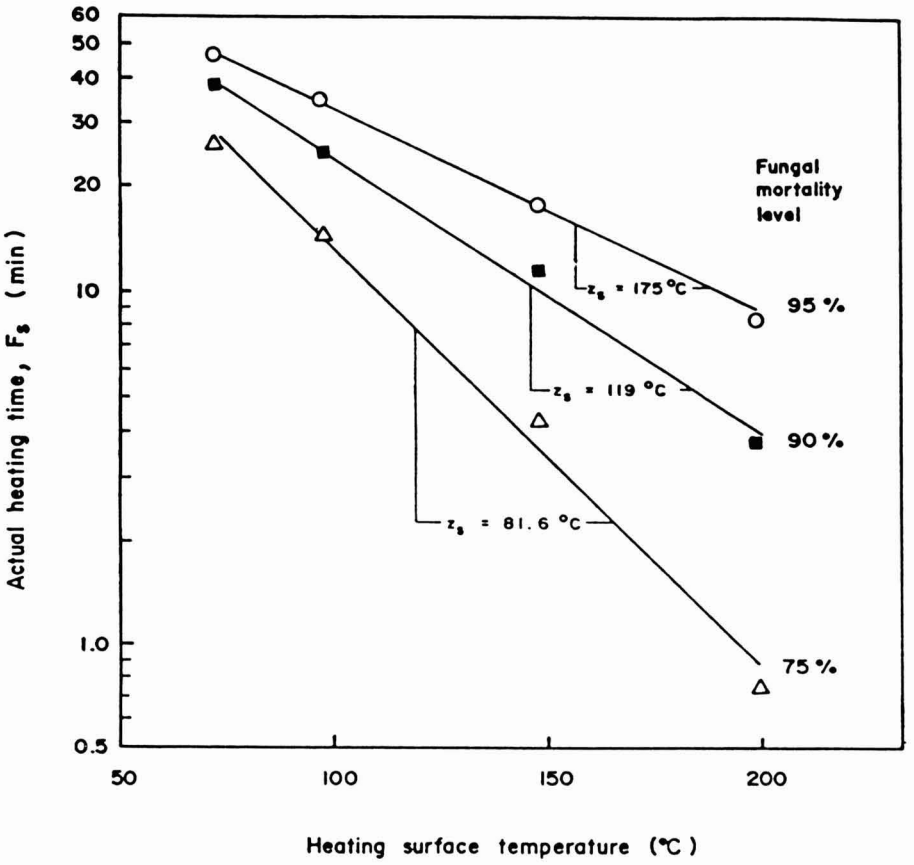

FIG. 6 ACTUAL HEATING TIME AS A FUNCTION OF HEATING SURFACE TEMPERATURES FOR VARIOUS FUNGAL MORTALITY LEVELS

Heating of high moisture rice using a 200°C surface temperature for about 3.5 min resulted in a 90% reduction of fungal load ratio. The same levels of fungal inactivation could be accomplished by heating the grain using 150, 100, 75°C heating surface temperatures for 13, 25 and 36 min, respectively. These heat treatments will also reduce the moisture content of rice by approximately 2 to 3% w.b. The amount of reduction increases with the heating surface temperature. The bulk grain temperatures corresponding to heating surface temperatures of 75 and 200°C were 60 and 85°C, respectively. These experimental results are based on the freshly harvested rough rice at an initial moisture content of about 26% (w.b.). Rough rice with lower moisture contents would probably heat at a faster rate, and require shorter exposure durations for a given fungal inactivation level. The estimated exposure times and temperatures are only applicable to the

TABLE 4.
REGRESSION COEFFICIENTS OF EQ. (6) RELATING F_s-VALUES WITH HEATING SURFACE TEMPERATURE AT VARIOUS LEVELS OF FUNGAL MORTALITY

Fungal mortality (%)	a_0	a_1	R^2	SEE	z_s* (°C)
75	2.4039	-0.0123	0.914	0.300	81.6
90	2.2678	-0.0084	0.969	0.101	119.0
95	2.1289	-0.0057	0.998	0.015	175.0

* $z_s = 1/a_1$

experimental heating used in this study. A general approach for representing thermal inactivation of fungi in high moisture rice based on the bulk grain temperature history is presented in the following section.

Generalized Representation of Thermal Inactivation of Fungi in High Moisture Rice

A procedure was developed for representing thermal inactivation of fungi in high moisture rice based on bulk grain temperature history in any given heat application equipment. This necessitated the computation of new z-values at some arbitrarily selected reference bulk grain temperatures. Accordingly equivalent exposure times which assumed no lags in the heating process were computed using an iterative procedure similar to the one proposed by Hayakawa *et al.* (1977) to solve the following equation (Bigelow 1920):

$$F_B = \int_0^t 10^{[\,T(t) - T_B\,]/z_B}\, dt \qquad (8)$$

Where F_B = equivalent exposure time at a reference bulk grain temperature to achieve a specified fungal mortality level, min
$T(t)$ = bulk grain temperature at any given time t, °C
T_B = reference bulk grain temperature, °C
z_B = inverse of the slope of the thermal death time curve based on bulk grain temperature, °C

The solution scheme (diagrammed in Fig. 7) included the following steps:

(1) Assume a z_B-value and from the time-temperature curves of bulk grain (Eq. 4) for known heating durations and fungal load reduction levels, compute the equivalent exposure time (Eq. 8) in each case by arbitrarily selecting different reference bulk grain temperatures (T_B).

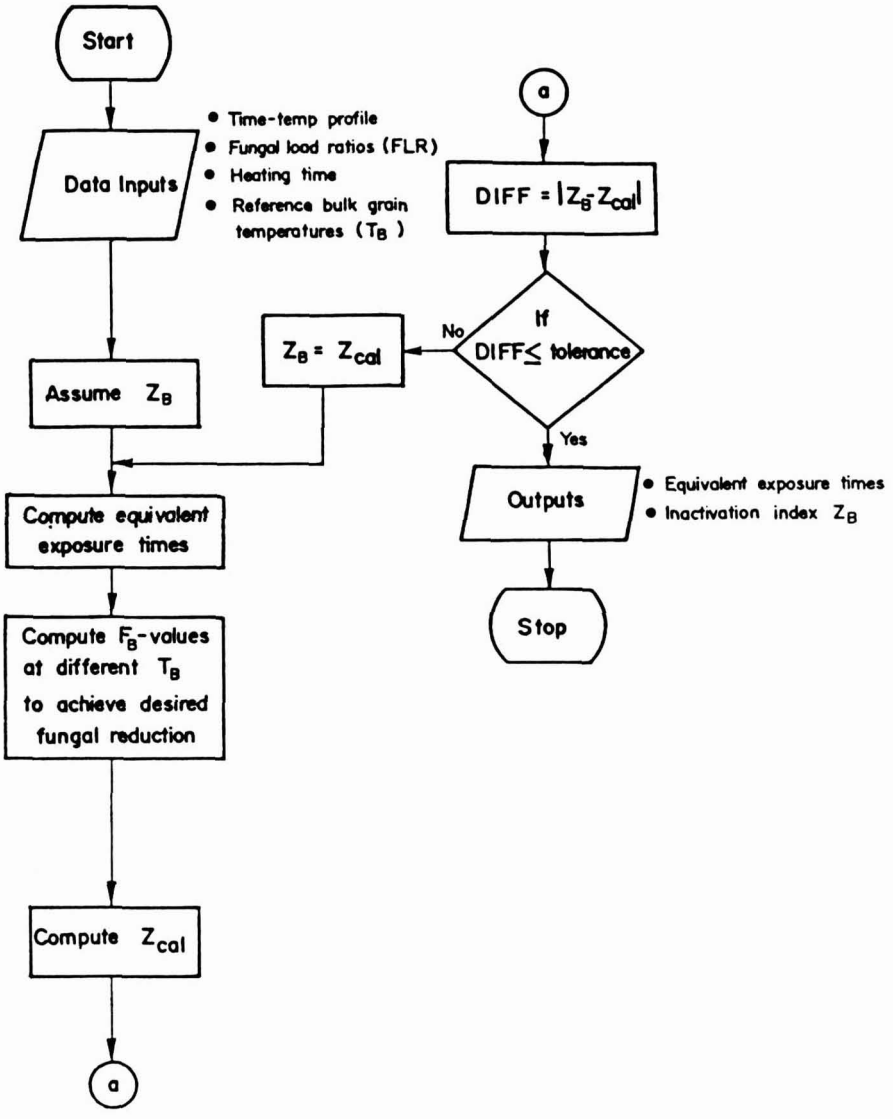

FIG. 7 FLOWCHART FOR DETERMINING z_B-VALUE

(2) Plot the fungal load ratio against the equivalent exposure time and compute the exposure time (F_B-values) corresponding to a desired level of reduction in fungal load ratio for each reference bulk grain temperature.

(3) Plot the common logarithm of time (F_B-values) determined at Step 2 against reference bulk grain temperature (T_B) and determine the slope of the relationship

by regression. Compute the reciprocal of the slope to give a z_B-value (z_{cal}). Compare the computed z_B-value with the assumed z_B-value used at Step 1. Set z_B equal to z_{cal} and repeat Steps 1, 2 and 3 until the assumed z_B-value becomes almost equal to the computed z_B-value.

The plots of equivalent exposure time (F_B-values) against reference bulk grain temperature (T_B) obtained from the iterative procedure for 75, 90 and 95% fungal mortality levels are shown in Fig. 8. These relationships were represented by the following equation:

$$\text{Log} \quad F_B = b_0 + b_1 T_B \tag{9}$$

Where b_0 and b_1 are regression coefficients (Table 5).

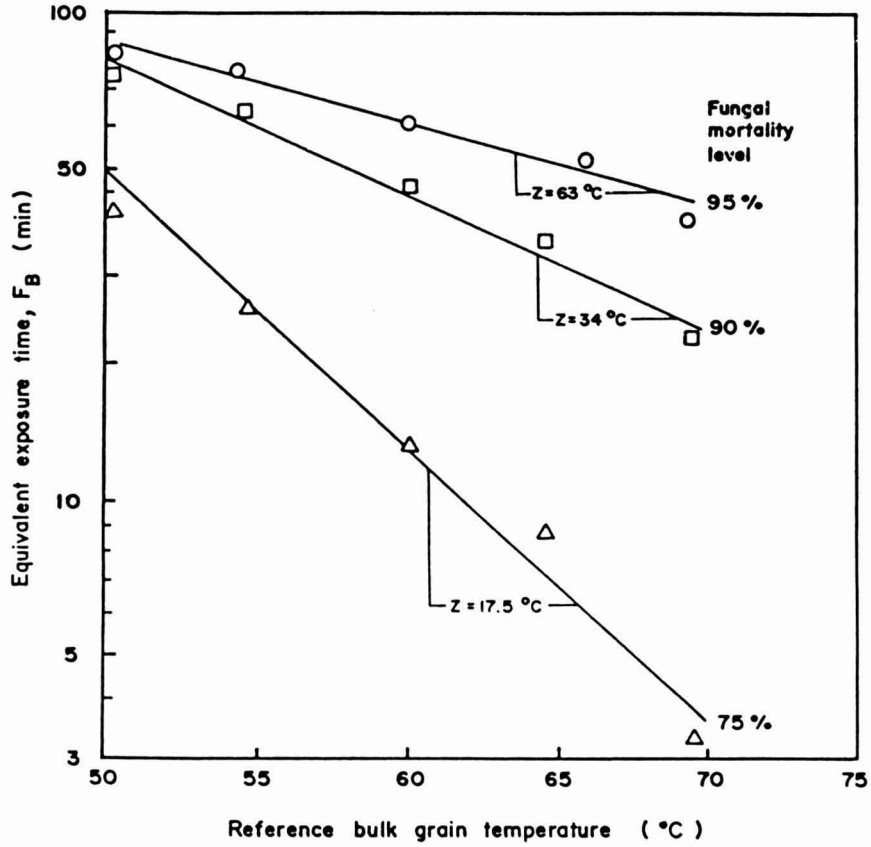

FIG. 8 EQUIVALENT EXPOSURE TIME AS A FUNCTION OF REFERENCE BULK GRAIN TEMPERATURE FOR VARIOUS FUNGAL MORTALITY LEVELS

TABLE 5.
REGRESSION COEFFICIENTS OF EQ. (9) RELATING EQUIVALENT EXPOSURE TIME (F_B) TO REFERENCE BULK GRAIN TEMPERATURE FOR VARIOUS FUNGAL MORTALITY LEVELS

Fungal mortality levels (%)	b_0	b_1	R^2	SEE	z_B* (°C)
75	4.5600	-0.0571	0.860	0.380	17.5
90	3.3767	-0.0291	0.850	0.200	34.0
95	2.7214	-0.0159	0.860	0.100	63.0

* $z_B = 1/b_1$

The inverse of the slope, $1/b_1$, led to the determination of z_B-values for selected fungal mortality levels as shown in Fig. 8.

Figure 8 shows the isothermal heating times (F_B-values) required to achieve various fungal mortality levels assuming no heating and cooling lags. A 90% reduction in fungal load could be achieved by heating the bulk grain either to 50°C for 82 min or to 70°C for 22 min. The computed values of F_B and z_B could be used in estimating the actual heating time from Eq. 8 for thermal inactivation of fungi in high moisture rice based on its time-temperature history during conduction heating with any given equipment.

SUMMARY AND CONCLUSIONS

This study showed that high-temperature short-time conduction heating of freshly harvested high moisture rice could effectively reduce its fungal population. A reduction in fungal activity of high moisture rice could prolong its temporary storage without quality deterioration prior to final drying of grain to safe moisture content.

Specific conclusions based on the results of this study are:

(1) Heat treatments reduced the fungal load in freshly harvested high moisture rice. The effectiveness of conduction heating for fungal inactivation depended upon the heating surface temperature and exposure time.

(2) It was possible to generalize the time-temperature requirements for arresting the fungal growth in rough rice in terms of the kinetic parameters analogous to those commonly used in thermal processing calculations based on the time-temperature history of bulk grain. Such a procedure also accounted for the heating and cooling lags usually encountered during heating in a given type of equipment.

(3) The measurement of carbon dioxide provided a simple alternative of estimating fungal load in high moisture rough rice.

ACKNOWLEDGMENTS

The financial support of United States Agency for International Development, Grant No. 936-5542 for the research project "Heat Sterilization and Accelerated Drying of High Moisture Rice for Safe Storage" is gratefully acknowledged.

REFERENCES

AYERST, G. 1969. The effects of moisture and temperature on growth and spore germination in some fungi. J. stored Products Res. *5*, 127–141.

BALL, C. O. and OLSON, F.C.W. 1957. *Sterilization in Food Technology*. McGraw-Hill Book Co., New York.

BIGELOW, W. D., BOHART, G. S., RICHARDSON, A. C. and BALL, C. O. 1920. Heat penetration in processing canned foods. Bulletin no. 16-L, Res. Lab. Natl. Canners Assn. Washington D.C.

BRADSHAW, J. G., STELMA, G. N., JONES, V. I., PEELER, J. T., WIMSATT, J. T., CORWIN, J. J. and TWEDT, R. M. 1982. Thermal inactivation of *Clostridium perfringens* entrotoxin in buffer and chicken gravy. J. Food Sci. *47*, 914–916.

CALDERWOOD, D. L. 1966. Use of aeration to aid drying. Trans. Amer. Soc. Agri. Eng. *9* (6), 893–895.

CALDERWOOD, D. L. and SCHROEDER, H. W. 1975. Chemical preservatives for maintaining moist rice in storage. Texas Agricultural Experiment Station Progress Report, 6 p.

CHANCELLOR, W. J. 1968. A simple grain drier using conducted heat. Trans. Amer. Soc. Agri. Eng. *11* (6), 857–862.

CHRISTENSEN, C. M. and KAUFMANN, H. H. 1974. Microflora. In *Storage of Cereal Grains and Their Products*, (C. M. Christensen, ed.) pp.158–193, AACC Inc., St. Paul, Minn.

DE PADUA, D. B. 1965. High moisture storage of rough rice by controlled environmental gas. Ph.D. Thesis, Michigan State University, East Lansing, U.S.A.

FAZLI, S.F.I. and SCHROEDER, H. W. 1966a. Kernel disinfection of Bluebonnet 50 rice by *Helminthosporium oryzae*. Phytopathology. *56*, 507–509.

FAZLI, S.F.I. and SCHROEDER, H. W. 1966b. Effect of kernel disinfection of rice by *Helminthosporium oryzae* on yields and quality. Phytopathology. *56*, 1003–1005.

FERNANDEZ, A., STROSHINE, R. and TUITE, J. 1985. Mold growth and carbon dioxide production during storage of high moisture corn. Cereal Chem. *62*, 137–143.

FLANNIGAN, B. 1977. Enumeration of fungi and assay for ability to degrade structural and storage components of grain. In *Biodeterioration Investigation Techniques*, (H. Walters, ed.) pp. 185–199, Applied Science Publishers.

HAYAKAWA, K., TIMBERS, G. E. and STIER, E. F. 1977. Influence of heat treatment on the quality of vegetables: organoleptic quality. J. Food Sci. *42*, 1286–1289.

HOLDSWORTH, S. D. 1985. Optimization of thermal processing—A Review. J. Food Eng. *4*, 89–116.

HYDE, M. B. 1969. Hazards of storing high moisture grain in airtight silos in tropical countries. Trop. Stored Products Inform. *18*, 9–12.

ILAG, L. L. 1982. Microorganisms in on-farm paddy deterioration studies. In *Paddy Deterioration in Humid Tropics*, pp. 57–59, German Agency for Technical Cooperation (GTZ), Eschborn, West Germany.

IWASAKI, T. and TANI, T. 1967. Effect of oxygen concentration on brown rice composition on deteriorative mechanisms of rice during storage. Cereal Chem. *44* (3), 233–237.

KREYGER, J. 1963. General considerations concerning the storage of seeds. Proc. Intl. Seed Testing Asso. *28*, 827–836.

LIN, J. T. 1985. Characterization of fungal invasion in paddy. M. Eng. Thesis, Asian Institute of Technology, Bangkok, Thailand.

MENDOZA, E. E., RIGOR, A. C. and ABITAL, F. L. 1981. Grain Quality deterioration in on-farm level operation. Paper presented at the Regional Grains Post-Harvest Workshop, Manila, Philippines, Jan. 20–22, 1981.

QUITCO, R. T. 1982. Studies on fungal infections and heating of paddy. In *Paddy Deterioration in Humid Tropics*, pp. 52–56, German Agency for Technical Cooperation (GTZ), Eschborn, West Germany.

REYES, JR., V. G. 1986. Heat treatment of high moisture paddy for temporary storage. D. Eng. Thesis, Asian Institute of Technology, Bangkok, Thailand.

ROOT, W. L. and COOK, E. M. 1980. Energy use in paddle dryers. In *Drying '80*, Vol. 2, (A. S. Majumdar, ed.) pp. 158–162. McGraw-Hill, New York.

SAUER, D. B. and BURROUGHS, R. 1974. Efficacy of various chemicals as grain mold inhibitors. Trans. Amer. Soc. Agri. Eng. *17*, 557–559.

SCHROEDER, H. W. 1967. Milling quality of Belle Patna Rice in experimental storage: A study on the effect of field fungi on subsequent invasion by storage fungi. J. stored Prod. Res. *3*, 29–33.

SCHROEDER, H. W. and SORENSON, J. W. 1961. Mold development in rough rice as affected by aeration during storage. The Rice J. *64* (7), 6–12 & 21–23.

STEELE, J. L., SAUL, R. A. and HUKILL, W. V. 1969. Deterioration of shelled corn as measured by carbon dioxide production. Trans. Amer. Soc. Agri. Eng. *12*, 685–689.

TATSUMO, T. 1963. Biochemical research on the toxic substance of rice yellowed by *P. islandicum*. Proc. Phar. *18*, 180.

COMPUTER SIMULATION OF MICROBIAL GROWTH DURING FREEZING AND FROZEN FOOD STORAGE

M. E. CASTELL-PEREZ[1], D. R. HELDMAN[2] and J. F. STEFFE[1]

[1]*Dept. of Agricultural Engineering*
Dept. of Food Science and Human Nutrition
Michigan State University
East Lansing, MI 48824

and

[2]*National Food Processors Association*
Washington, D. C.

Accepted for Publication July 19, 1988

ABSTRACT

A computer simulation model was developed to predict the time for temperature equilibration as well as microbial growth within a food product during freezing and the equilibration to frozen storage conditions. Theoretical results indicate that freezing medium temperature, surface heat transfer coefficient and product size influence the equilibration time significantly. Storage conditions influenced the equilibration time during storage and significantly influenced the growth of microorganisms. Microbial growth is a function of the freezing time. Slow freezing of a food product from a high initial temperature and stored at a relatively high temperature can provide conditions for microbial growth as compared to very rapid freezing processes. The model is a useful tool for approximate indications of effects of freezing conditions on microbial growth within a food product.

INTRODUCTION

Most freezing design computations require determination of refrigeration requirements and/or freezing times for the product. For time periods after completion of the freezing process, the temperature equilibration period required to achieve storage temperature may be of importance in terms of the final product quality as well as process efficiency. Knowledge of the influence of freezing process parameters on the food product should reduce energy consumption as well as improve quality of the product during storage (Lee and Toledo 1984;

Journal of Food Process Engineering 10 (1989) 249-268.

Buchanan 1986). The equilibration period may also have a significant influence on product quality from the microbiological standpoint because sub-zero temperatures do not necessarily inactivate microorganisms (Castell-Perez 1984; Buchanan 1986).

The objectives of this research were:

(1) To develop a computer simulation model to predict the time for temperature equilibration as well as microbial growth within a food product during the freezing and the temperature equilibration periods.
(2) To discuss the influence of parameters on equilibration times and microbial growth during freezing and equilibration.

THEORETICAL CONSIDERATIONS

A computer program was developed for this investigation as follows:

(1) To predict temperature distribution within a food product of infinite slab, infinite cylinder and spherical geometry during freezing.
(2) To predict temperature profiles during the temperature equilibration period after freezing is stopped.
(3) To predict microbial growth within the frozen product during the freezing and equilibration periods.

The criteria for freezing time was based on area average enthalpy for infinite geometries and a volume average enthalpy for the sphere. The criteria was established by the time when the average enthalpy reached a value equivalent to $-20°C$ ($-4°F$). At this point, the freezing process simulation was stopped. The volume average enthalpy approach was utilized by Heldman and Gorby (1975) for spherical geometry with excellent results. The area average enthalpy is expressed as

$$H_A = \frac{1}{A} \int_A H \, dA \tag{1}$$

while the volume average enthalpy is

$$H_V = \frac{1}{V} \int_V H \, dV \tag{2}$$

Other investigations have also used enthalpy-based approaches (Sastry 1984; Mannapperuma and Singh 1988). Improvement of techniques for prediction of

freezing times continues to be of major interest for researchers; a variety of numerical methods for prediction of freezing times have been developed and analyzed (Cleland and Earle 1984a, 1984b; Ramaswamy and Tung 1984; Succar and Hayakawa 1984; Abdulla and Singh 1985; Cleland *et al.* 1986; Nomino and Hayakawa 1986; Pham 1986, 1987). Analytical methods were also analyzed (Hayakawa *et al.* 1986; Ilicali and Saglam 1987).

The prediction model for freezing times is based on the model initially developed by Lescano (1973) and later improved by Heldman and Gorby (1975). The Fourier heat conduction equation is the governing differential equation for heat conduction in isotropic systems. For one-dimensional heat transfer in a homogeneous infinite slab, the equation is

$$Cp(T)\ \rho\ (T)\frac{\partial T}{\partial t} = \frac{\partial}{\partial x}\left[k_x(T)\ \frac{\partial T}{\partial x}\right] \tag{3}$$

This equation represents the transient-state heat conduction in the product. Thermal properties are dependent on temperature and vary with time. Similar equations for cylindrical and spherical geometries were used. The unique feature of this model is related to the accurate prediction of temperature dependent thermal properties of the food below the initial freezing point. Only the thermal properties of the unfrozen product are required as input.

Initial and Boundary Conditions

Initial Conditions:

The product is at uniform temperature initially.

Boundary Conditions:

$$\left.\frac{\partial T}{\partial x}\right|_{x=0} = 0 \qquad \text{at} \quad x = 0 \tag{4}$$

(for slab)

$$\left.\frac{\partial T}{\partial r}\right|_{r=0} = 0 \qquad r = 0 \tag{5}$$

(for cylinder and sphere)

$$k_x(T)\ \frac{\partial T}{\partial x} + h_c\ (T - T_\infty) = 0 \tag{6}$$

at the convective surface and $t \geq 0$
(for slab)

$$k_r\ (T)\ \frac{\partial T}{\partial r} + h_c\ (T - T_\infty) = 0 \qquad (7)$$

(for cylinder and sphere)

Assumptions

(1) The freezing medium temperature and the product initial temperature are constant and uniform.
(2) The surface heat transfer coefficient (h_c) remains constant during the freezing process (convective boundary condition).
(3) Heat transfer from the freezing medium to the product occurs by convection and heat conduction occurs within the product.
(4) Heat transfer occurs only in the x-direction for a slab and in the r-direction for a cylinder and a sphere.
(5) Moisture loss (water vapor transport from the product surface to the air) is negligible.
(6) Thermal properties above the initial freezing temperature are constant.
(7) Overall product composition does not change during the freezing process.

Temperature Equilibration Time Prediction Model

Temperature fluctuations in stored frozen foods have been studied by Zuritz and Singh (1985) and the effects of packaging materials on the temperature fluctuations by Zuritz and Sastry (1986).

The approach developed by Heldman and Gorby (1975) for prediction of temperature history during storage conditions for a spherical product was modified to account for product shape.

To develop the simulation model, the following input parameters were needed: area average enthalpy as determined by Eq. (1), temperature history of product during freezing (output from freezing time prediction model), surface heat transfer coefficient and storage temperature.

The initial and boundary conditions during equilibration are:

Initial condition:

$$T = T_o' \text{ at } t_e = 0 \qquad (8)$$

Boundary Conditions:

$$k_x (T) \frac{\partial T}{\partial x} + h_c' (T - T_{st}) = 0 \quad (9)$$

at the convective surface and $t_e \geq 0$ (slab)

$$k_r (T) \frac{\partial T}{\partial r} + h_c' (T - T_{st}) = 0 \quad (10)$$

for cylinder and sphere

The storage conditions considered included a surface heat transfer coefficient (h_c) of 1 W/m^{2}C and a medium temperature (T_{st}) of -20°C (-4°F) which are representative of the storage conditions for frozen beef. With these new variables, the computer program predicted the temperature distribution within the product until the surface temperature equaled the medium temperature. At this point, the simulation stops. Output from this model is utilized to predict microbiological populations within the frozen product during freezing and frozen storage.

Microbial Growth Prediction Model

Many researchers have discussed the kinetics of microbial growth and attempted to express it mathematically. Kinetics models based on the Arrhenius equation have been used for microorganisms (Pirt 1975; Thompson and Busta 1981) and inactivation (Pflug 1968; Thompson *et al.* 1979). Effectiveness of packaging was also modelled by Zaura and Zaritzky (1985).

Kono (1968) derived the growth rate equation from the standpoint of chemical reaction kinetics for each phase of microbial population growth. Only the *exponential phase* of growth is considered in this investigation:

$$N = N_O \exp (Kt) \quad (11)$$

The following information was needed for the simulation: output from freezing and equilibration temperature distribution program (for each geometry); initial microbial population; growth rate constant (K) versus temperature relationship; and product dimensions (height, width and length of slab; radius and height of cylinder; radius of sphere).

Mass Average Population Criteria

The criteria of mass average population consisted of the calculation of the distribution of microbial population within the total mass of the product. The subdivision of the product into volume elements facilitates computer iteration and a sequence of calculations are performed for each volume element to obtain the final population. This method was originally developed by Teixeira *et al.* (1969) for calculation of lethality.

RESULTS AND DISCUSSION

Results from simulation were obtained by running the computer program with different input parameters. The influence of several input parameters was analyzed. Figures 1 and 2 illustrate the temperature distribution within the food product during the freezing process and the temperature equilibration period following freezing. Temperature distribution curves showed good agreement with previous works such as Lescano (1973).

Figure 1 presents the temperature distribution at the end of a very rapid freezing process (high surface heat transfer coefficient, low freezing medium temperature) for an infinite slab. It is clear that the rapid freezing conditions cause a rapid decrease of the surface temperature (-110°C) while the center temperature is still relatively high (9°C) when the freezing process ends. Consequently, the equilibration of temperatures requires a long period of time due to the large temperature gradient between the product center and the product surface. The equilibration of temperatures occurs at a reduced rate compared to the freezing time.

The results in Fig. 2 show that the temperature decrease is more uniform within the product at the end of a very slow freezing process (low surface heat transfer coefficient, high freezing medium temperature). Less time is required for temperature equilibration as compared to Fig. 1. This is due to the similar temperatures at the product surface and center at the beginning of equilibration.

As demonstrated, freezing conditions influence the temperature distribution at the end of freezing. The influence of these conditions on freezing time has been discussed by Heldman (1974), Heldman and Gorby (1975), Purwadaria (1980), Cleland and Earle (1984b), Succar and Hayakawa (1984) and Ramaswamy and Tung (1984). The influence on the time for temperature equilibration after freezing is closely related to the temperature distribution at the end of freezing.

The freezing conditions have a dramatic influence on the temperature distribution at the end of freezing process and, consequently, on the time for temperature equilibration. Differences in product geometry are due to the different volume/area ratios, with the sphere having the lower freezing times (Fig. 3).

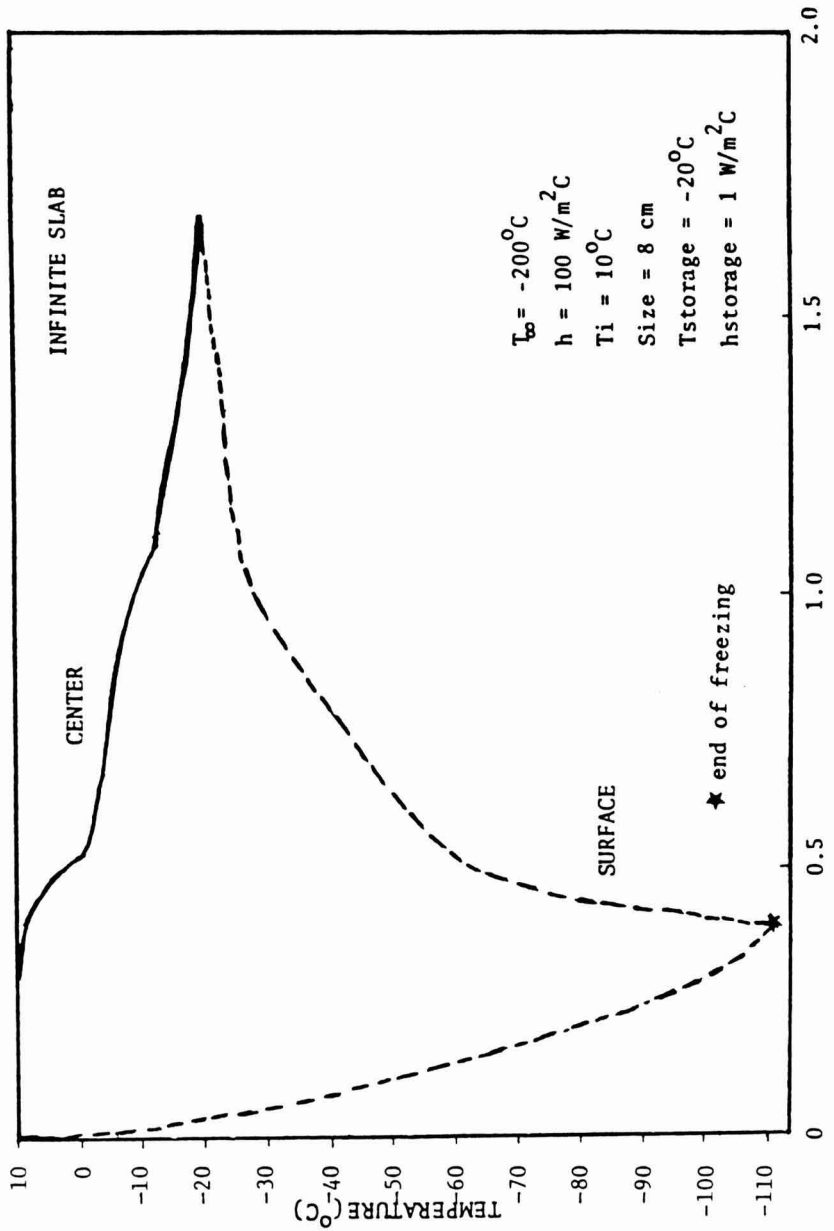

FIG. 1. TEMPERATURE DISTRIBUTION WITHIN THE FOOD PRODUCT DURING VERY RAPID FREEZING AND EQUILIBRIUM

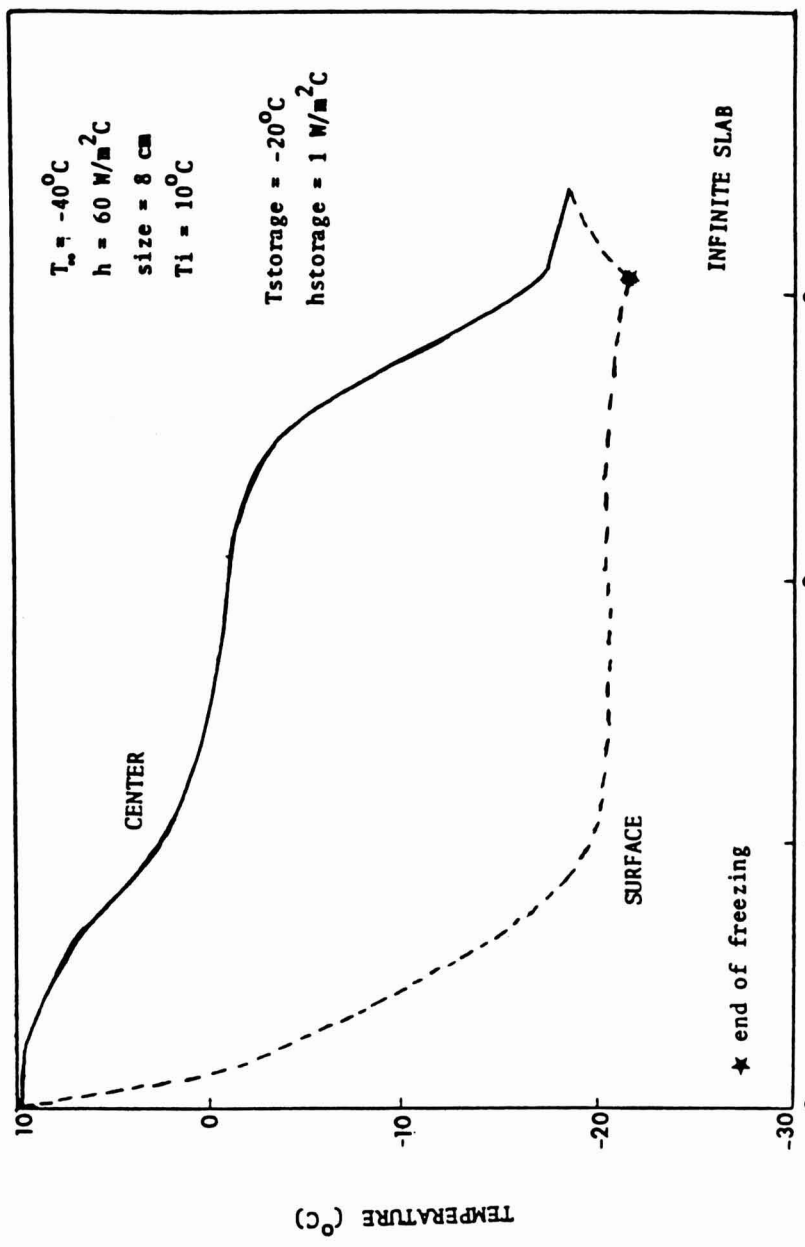

FIG. 2. TEMPERATURE DISTRIBUTION WITHIN THE FOOD PRODUCT DURING SLOW FREEZING AND EQUILIBRIUM

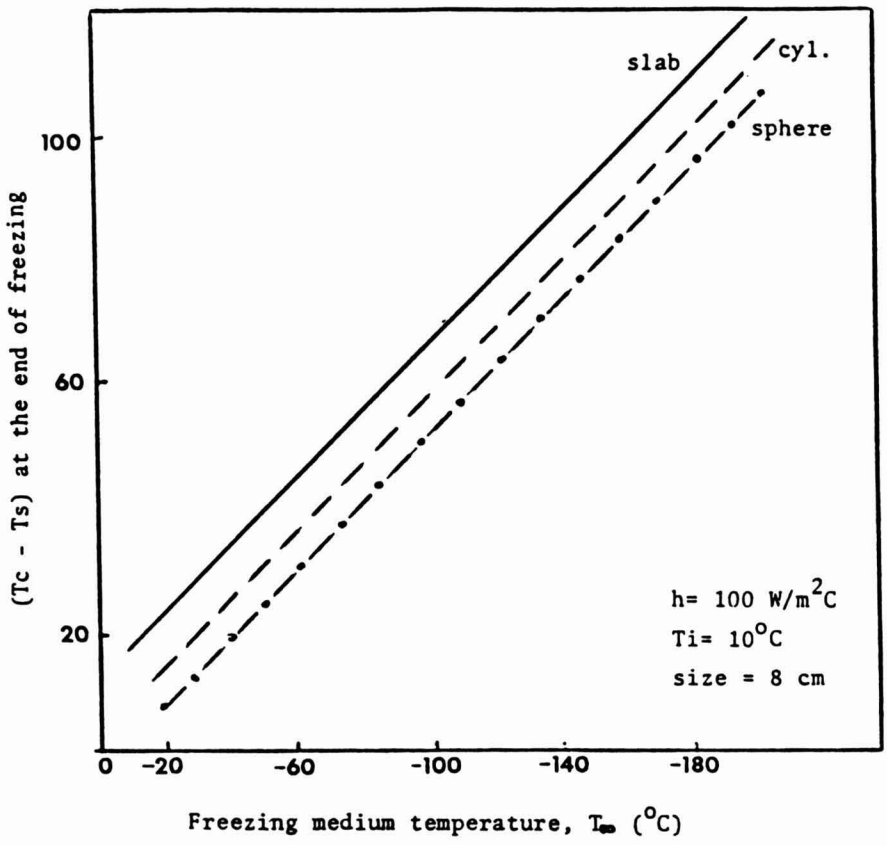

FIG. 3. TEMPERATURE DISTRIBUTION AT THE END OF FREEZING VERSUS FREEZING MEDIUM TEMPERATURE

Temperature Equilibration Time

The temperature equilibration time was defined as the time from the end of the freezing process for the product surface and center temperatures to reach the storage temperature. Consequently, the time for temperature equilibration after the freezing process is a function of the temperature distribution within the product at the end of freezing. It was observed that the larger the temperature gradient, the longer the time to achieve temperature equilibration (Fig. 4). This effect is significant and could be of concern when considering the potential for microbial growth during extended periods of elevated temperature.

Storage conditions also influence the time for temperature equilibration after freezing: higher values of the surface heat transfer coefficient will lead to more rapid equilibration of temperatures within the product. The influence of the

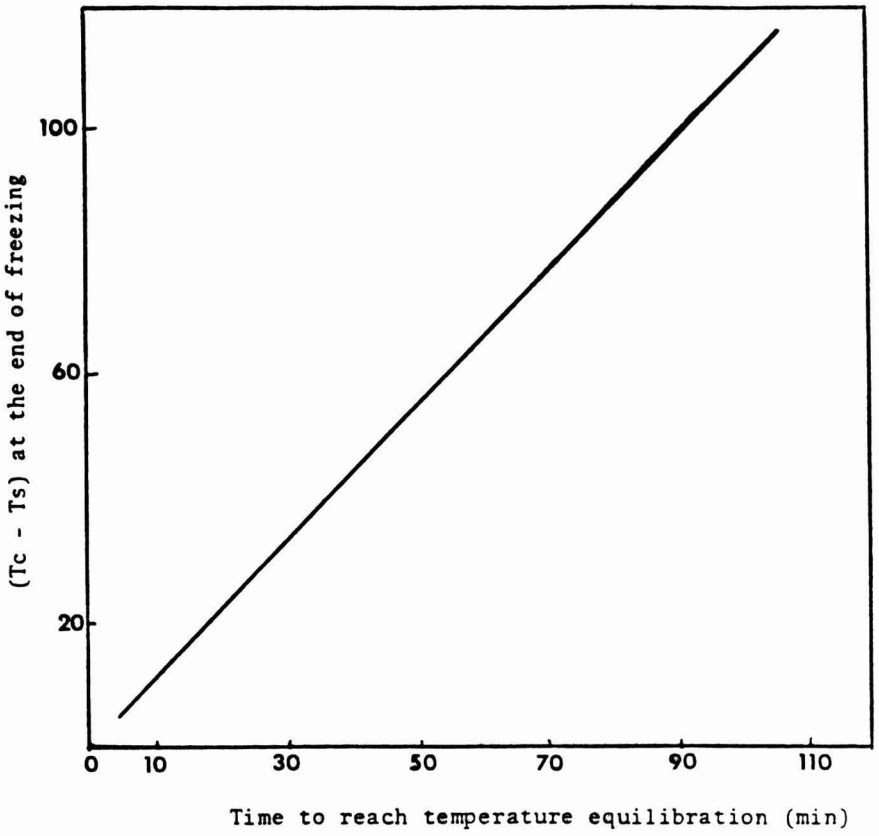

FIG. 4. TEMPERATURE DISTRIBUTION WITHIN THE PRODUCT AT THE END OF FREEZING VERSUS TIME TO REACH TEMPERATURE EQUILIBRATION

temperature of storage on the time for temperature equilibration is related to the freezing conditions which are established for the center temperature to achieve a temperature equivalent to the storage temperature. This influences freezing time, and consequently, the temperature distribution within the product at the end of freezing.

Influence of Freezing Process and Storage Conditions on Product Quality (microbial growth)

A primary objective of this investigation was to predict the growth of selected microorganisms in ground beef during the freezing process and the selected frozen storage period. Growth of psychrophilic Bacillus was selected based on ability to observe growth at low temperature [below 0°C (32°F)] (Dultschaever *et al.* 1973; Goepfert and Kim 1975; Lee and Toledo 1984; Simard *et al.* 1984, Buchanan 1986).

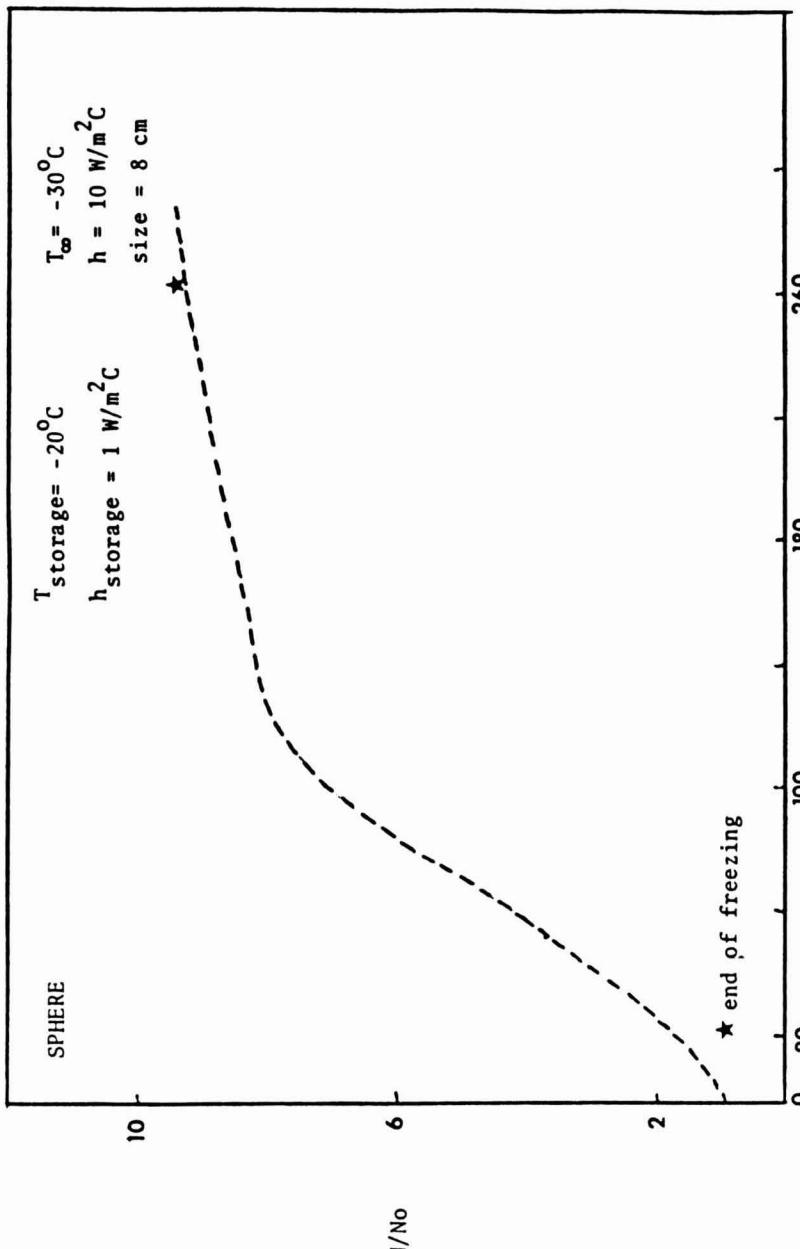

FIG. 5. MICROBIAL GROWTH DURING SLOW FREEZING CONDITIONS AND STORAGE

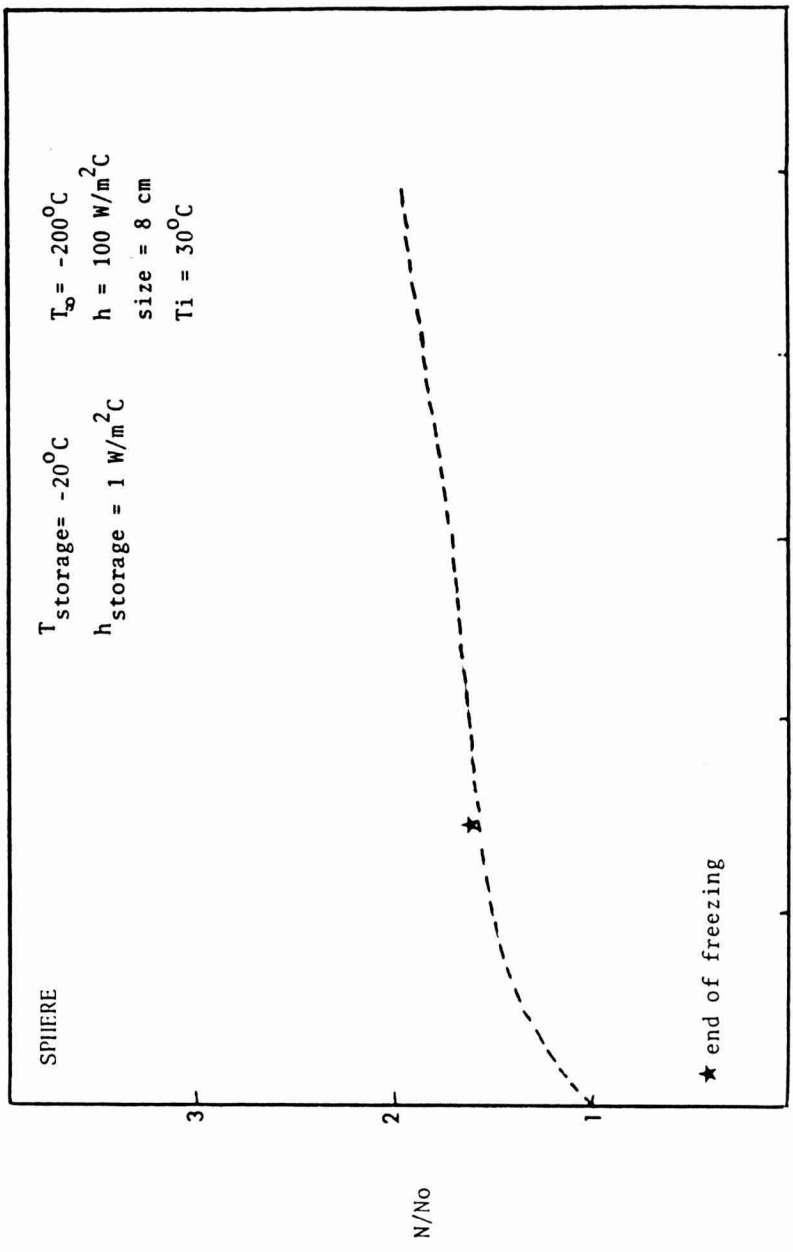

FIG. 6. MICROBIAL GROWTH DURING VERY RAPID FREEZING CONDITIONS AND STORAGE

The results (Fig. 5) illustrate the increase in microbial population during slow freezing conditions. The ratio of microbial populations (N/N_o) was plotted versus time. It is clear that slow freezing provides favorable conditions for microbial growth within a food product due to relatively high product temperatures during the freezing process. The increase in microbial population is more significant during the initial period of freezing and decreases gradually as the freezing process continues. Microbial growth is limited during rapid freezing because the product temperature is rapidly decreased (Fig. 6).

Prediction of microbial growth during different freezing conditions was conducted. Figure 7 illustrates the influence of freezing time on the extent of microbial growth within the product at completion of freezing. Slow freezing processes constitute a potential for the growth of certain microorganisms and

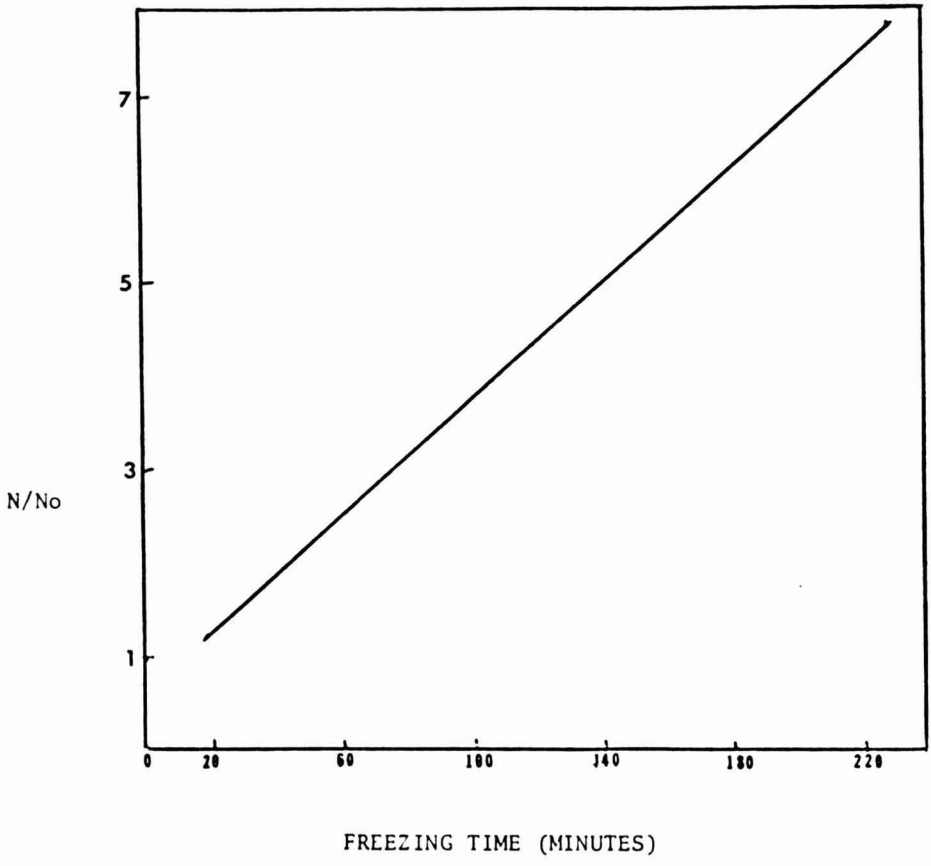

FIG. 7. PREDICTED MICROBIAL GROWTH AT THE END OF FREEZING VERSUS FREEZING TIME

this type of freezing process can be important in terms of final product quality. On the other hand, very rapid freezing processes do not provide favorable microbial growth conditions, probably due to the limited growth of nonpsychrophiles at low (below 0°C) temperatures.

Microbial Growth during Temperature Equilibration Period

Figure 8 presents the microbial growth during the temperature equilibration period following a slow freezing process. Although the time period is short, microbial growth still occurs to a moderate extent. Figure 9 presents the microbial growth during storage following rapid freezing conditions. In this case, temperature equilibration time is significant but microbial growth is moderate.

For rapid freezing conditions, the temperature at the center is sufficiently high to encourage increase of microbial populations. The influence on growth of microbial populations could be related more closely to the time for temperature equilibration than to temperature. In addition, high storage temperatures result in a significant increase in microbial population as compared to a lower storage temperature. Figure 10 illustrates the influence of the surface heat transfer coefficient during storage on microbial growth during equilibration. The higher values resulted in less microbial growth due to smaller time required to reach temperature equilibration. Large values of the surface heat transfer coefficient should reduce microbial growth during equilibrium and storage to negligible levels.

In conclusion, selection of the proper freezing and storage conditions is an important factor in preserving the quality of meat products due to the considerably long periods of time at which this food product is usually stored before consumption.

Application of Simulation Model in the Frozen Food Industry

The application of the simulation model in the food industry is for selection of the optimum freezing and storage conditions for a desired product, size, shape and quality characteristics. Input parameters may be varied in order to collect enough information for the development of a chart illustrating the relationships between freezing conditions and microbial growth within the product.

Some limitations of the model are:

(1) Only the influence of temperature on microbial growth was considered for simulation. Water activity (A_w) effects were not accounted for.
(2) Microbial growth rate constants (K) may be a function of substrate or product.
(3) Uniform microbial distribution within the product was assumed. Other factors affecting microbial growth such as nutrients, atmosphere, location within the object, and changes in concentration of solutes due to freezing, may influence the results from the theoretical simulation.

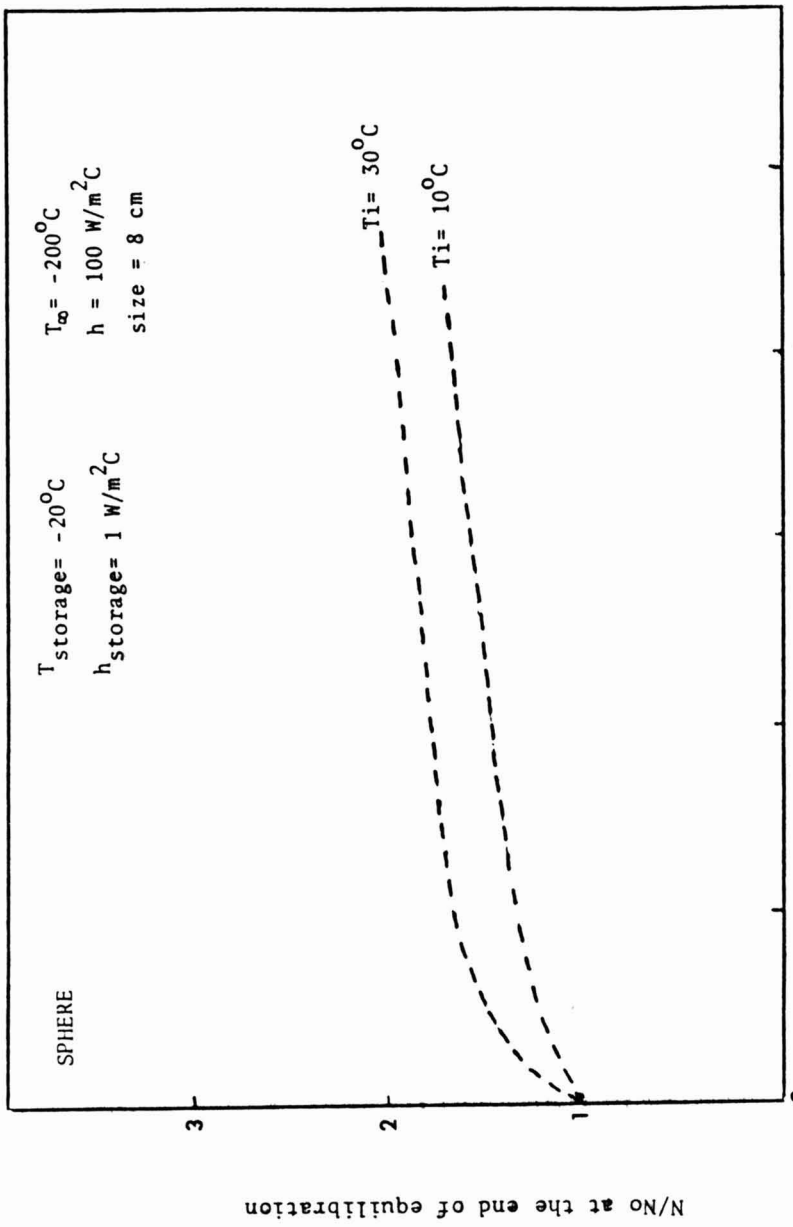

FIG. 8. MICROBIAL GROWTH DURING EQUILIBRATION PERIOD FOLLOWING A VERY RAPID FREEZING PROCESS.

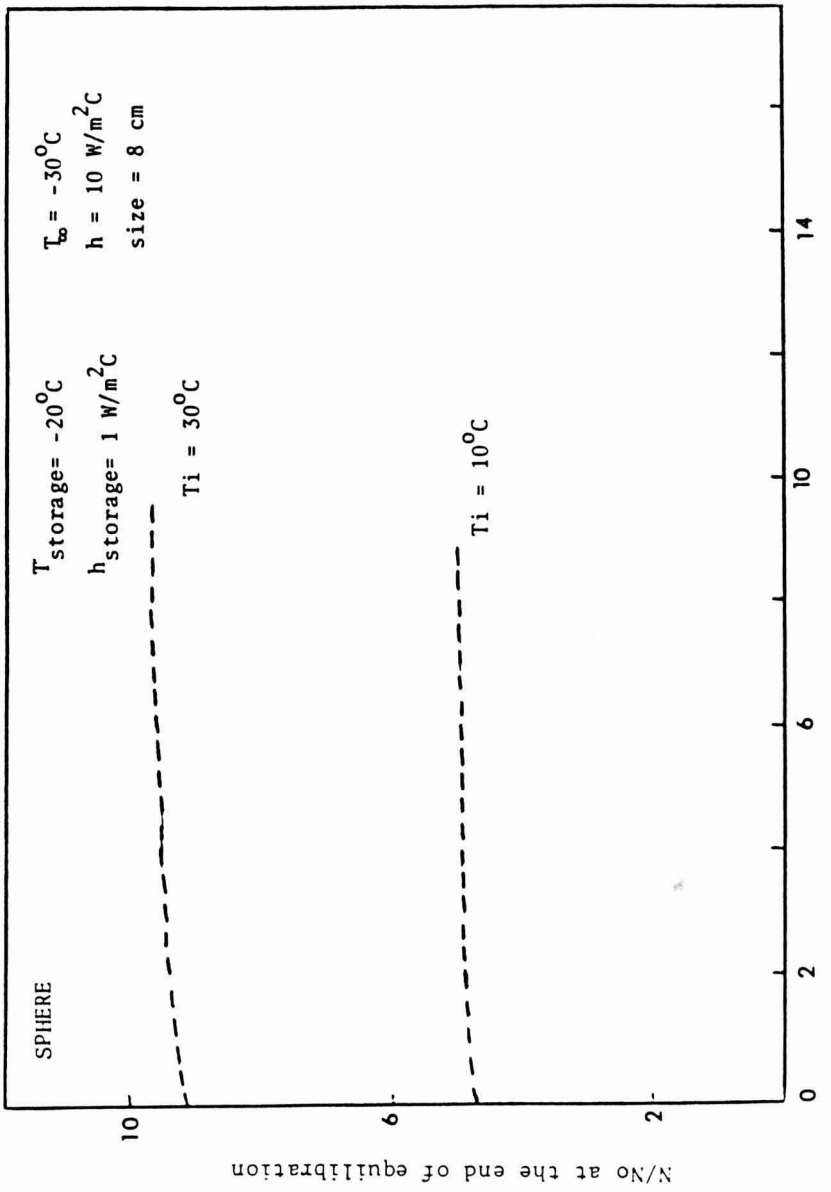

FIG. 9. MICROBIAL GROWTH DURING EQUILIBRATION PERIOD FOLLOWING A SLOW FREEZING PROCESS

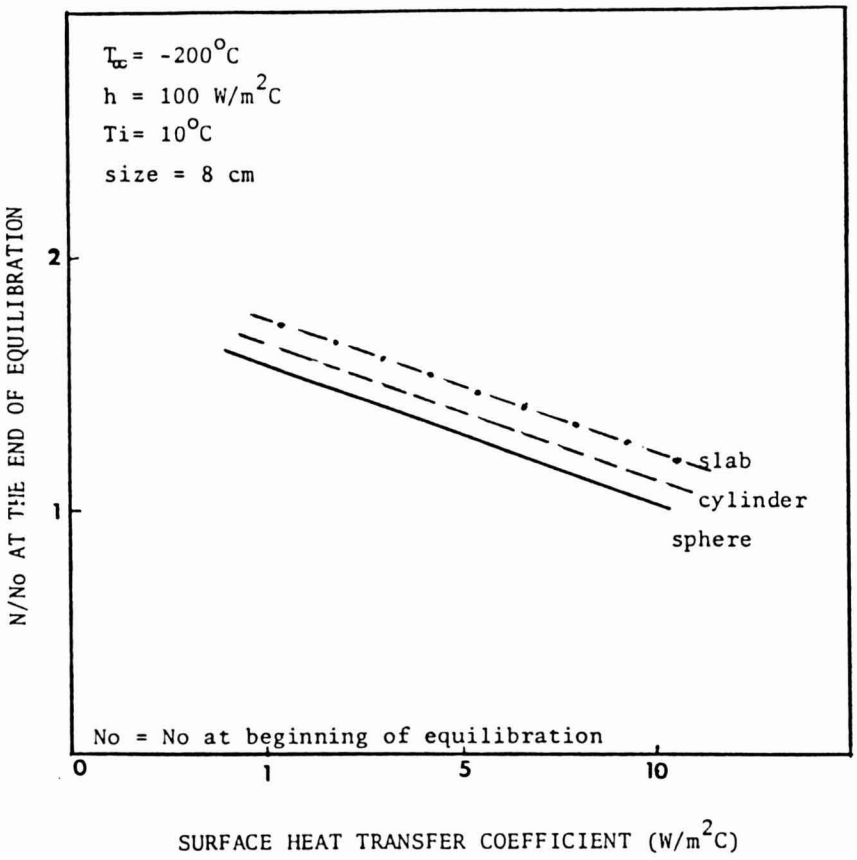

FIG. 10. PREDICTED MICROBIAL GROWTH AT THE END OF EQUILIBRATION VERSUS SURFACE HEAT TRANSFER COEFFICIENT DURING STORAGE

(4) Food products are nonhomogeneous and this is not accounted for in the theoretical simulation.

The practical implications of the problem of microbial growth within a food product during freezing and frozen storage initiated the development of this investigation. Experimental verification was not conducted and simulation results can only be considered as an approximate indication of the real situation.

CONCLUSIONS

(1) Freezing medium temperature, surface heat transfer coefficient, product size and storage conditions significantly influence the time for temperature equilibration and the growth of microorganisms in the food product. The extent

of microbial growth during freezing and temperature equilibration is influenced directly by freezing time.

(2) Initial product temperature has a significant influence on microbial growth during slow freezing processes. Slow freezing of a product initially at 30°C can result in a potential increase in microbial growth population of about 83% during freezing as compared to an increase of 4% when the product was initially at 10°C.

(3) Storage temperature has a significant influence on microbial growth during equilibration. Reducing the storage temperature from −20°C to −30°C provides a decrease of 20% in microbial population growth. An increase in storage temperature to −10°C would result in a microbial population increase of about 80% during the equilibration period.

(4) Results from the theoretical simulation indicate that slow freezing processes provide conditions for significant increases in microbial population and these conditions will be important in terms of product quality when initial microbial populations are high. Rapid freezing processes would be important under these conditions.

LIST OF SYMBOLS

A	area, m^2
A_w	Water activity
C_p	Specific heat of product, kJ/kg°C
ρ	Density of product, kg/m^3
h_c	Surface heat transfer coefficient in freezing, $W/m^2°C$
h'_c	Surface heat transfer coefficient in storage, $W/m^2°C$
H_A	Area average enthalpy, kJ/kg
H_V	Volume average enthalpy, kJ/kg
$k(T)$	Thermal conductivity of product, W/m°C
K	Growth rate constant, min^{-1}
N	Microbial population at time t, cells/g
N_o	Initial microbial population, cells/g
r	Radius of cylinder or sphere, m
t	Time, minutes
t_e	Time during equilibration, minutes
T	Temperature, °C
T_c	Center temperature, °C
T_i	Product temperature at beginning of freezing, °C
T_o'	Product temperature at end of freezing and beginning of equilibrium, °C
T_s	Surface temperature, °C
T_{st}	Storage temperature, °C

T_∞	Freezing medium temperature, °C
V	Volume, m^3
x	Thickness of slab, m

REFERENCES

ABDALLA, H. and SINGH, R. P. 1985. Simulation of thawing of foods using finite method. J. Food Proc. Eng. *7*(4), 273.

BUCHANAN, R. L. 1986. Processed meats as a microbial environment. Food Technol. *40,* 134.

CASTELL-PEREZ, M. E. 1984. Computer simulation of microbial quality of a food product during freezing and frozen storage. M.S. Thesis. Agricultural Engineering Department, Michigan State University, East Lansing, MI.

CLELAND, A. C. and EARLE, R. L. 1984a. Assessment of freezing time prediction methods. J. Food Sci. *49*(4), 1034.

CLELAND, A. C. and EARLE, R. L. 1984b. Freezing time predictions for different final product temperatures. J. Food Sci. *49*(4), 1230.

CLELAND, A. C., CLELAND, C. J., EARLE, R. L. and BYRNE, S. J. 1986. Prediction of thawing times for foods of simple shape. Int. J. Ref. *9,* 220.

DE REINICK, A. R. and SCHWARTZBERG, H. 1986. Predicting temperature versus time behavior during the freezing and thawing of rectangular foods. Biotech. Prog. *2*(3), 164.

DULTSCHAEVER, C. L., ARNOTT, D. R. and BULLOCK, D. H. 1973. Bacteriological quality of raw refrigerated ground beef. J. Milk Technol. *36,* 375.

GOEPFERT, J. M. and KIM, H. U. 1975. Behavior of selected foodborne pathogens in raw ground beef. J. Milk Food Technol. *38,* 449.

HAYAKAWA, K., SCOTT, K. D. and SUCCAR, J. 1986. Theoretical and semi-theoretical methods for estimating freezing or thawing time. ASHRAE Trans. *91*(2), 371.

HELDMAN, D. R. 1974. Computer simulation of food freezing processes. Proceedings of the VI Int. Congress of Food Science and Technology. *IV,* 397.

HELDMAN, D. R. and GORBY, P. 1975. Computer simulation of individual-quick freezing of foods. ASAE, Paper No. 75-6016, ASAE, St. Joseph, MI 49085.

ILICALI, C. and SAGLAM, N. 1987. A simplified analytical model for freezing time calculation in foods. J. Food Proc. Eng. *9,* 299.

KONO, T. 1968. Kinetics of microbial cell growth. Biotech. Bioeng. *10,* 105.

LEE, C. M. and TOLEDO, R. T. 1984. Comparison of shelf-life and quality of mullet stored at zero and subzero temperature. J. Food Sci. *49*(2), 317.

LESCANO, C. E. 1973. Predicting freezing curves in codfish fillets using the ideal binary solution assumption. M.S. Thesis. Agricultural Engineering Department, Michigan State University, East Lansing, MI.

MANNAPPERUMA, J. D. and SINGH, R. P. 1988. Prediction of freezing and thawing times of foods using a numerical method based on enthalpy formulation. J. Food Sci. *53*(2), 626.

NOMINO, C. and HAYAKAWA, K. 1986. Thawing time of frozen food of a rectangular or finitely cylindrical shape. J. Food Sci. *51*(1), 116.

PFLUG, I. J. 1968. Evaluating the lethality of heat processes using a method employing Hick's table. Food Technol. *23*, 1153.

PHAM, Q. T. 1986. Simplified equation for predicting the freezing time of foodstuffs. J. Food Technol. *21*, 209.

PHAM, Q. T. 1987. Calculation of bound water in frozen food. J. Food Sci. *52*(1), 210.

PIRT, S. J. 1975. *Principles of Microbe and Cell Cultivation*. John Wiley & Son, New York.

PURWADARIA, H. K. 1980. A numerical prediction model for food freezing using finite element methods. PhD Thesis. Agricultural Engineering Department, Michigan State University, East Lansing, MI.

RAMASWAMY, H. S. and TUNG, M. A. 1984. A review on predicting freezing times of foods. J. Food Proc. Eng. *7*, 169.

SASTRY, S. K. 1984. Freezing time prediction: An enthalpy-based approach. J. Food Sci. *49*(4), 1121.

SIMARD, R. E., ZEE, J. and L'HEUREUX, L. 1984. Microbial growth in carcasses and boxed beef during storage. J. Food Prot. *47*, 773.

SUCCAR, J. and HAYAKAWA, K. 1984. Parametric analysis for predicting freezing time of infinitely slab-shaped foods. J. Food Sci. *49*(2), 468.

TEIXEIRA, A. A., DIXON, J. R., ZAHRADNIK, J. W. and ZINSMEISTER, G. E. 1969. Computer determination of spore survival distributions in thermally processed conduction-heated foods. Food Technol. *23*, 78.

THOMPSON, W. S., BUSTA, F. F., THOMPSON, D. R. and ALLEN, C. E. 1979. Inactivation of Salmonellae in autoclaved ground beef exposed to constantly raising temperatures. J. Food Prot. *43*(5), 410.

THOMPSON, D. R. and BUSTA, F. F. 1981. Modelling microbial populations during meat cooking and cooling. Trans. the ASAE, *23*, 664.

ZAURA, M. C. and ZARITZKY, N. E. 1985. Modeling of microbial growth in refrigerated packaged beef. J. Food Sci. *50*(4), 1003.

ZURITZ, C. A. and SINGH, R. P. 1985. Modeling temperature fluctuations in stored frozen foods. Int. J. Ref. *8*, 289.

ZURITZ, C. A. and SASTRY, S. K. 1986. Effect of packaging materials on temperature fluctuations in frozen foods: Mathematical model and experimental studies. J. Food Sci. *51*(4), 1050.

MATURITY STANDARDS FOR PROCESSING CLINGSTONE PEACHES

MICHAEL J. DELWICHE

Department of Agricultural Engineering
University of California
Davis, California 95616

Accepted for Publication September 9, 1988

ABSTRACT

The flesh color of 5 clingstone peach cultivars was measured (in CIELAB coordinates) by tristimulus colorimeter before and after canning. Before canning, fruit were separated into 3 color classes (1A: green-yellow, 4A: yellow-green, 7A: orange) by visual comparison with a trial maturity chart. After canning, flesh color was measured and visually graded. All samples in color class 1A were rated USDA grade C, while classes 4A and 7A were rated grade A. Flesh color was also measured as a function of time before and after harvest. Fresh flesh L values were approximately constant, a* values increased steadily, and b* values increased then slightly decreased. Final specifications for a new maturity chart were 7 colors of constant luminance (L* = 76.5) and linearly increasing a* and b* values (−5.0 to 13.0 and 70.1 to 76.4, respectively), corresponding to a time step of 3.5 days between colors.*

INTRODUCTION

A great majority of clingstone peaches in the US are grown and processed in California, with a 1986 fresh production of 408 million kg from 13,850 hectares. One critical factor determining grade and ultimate quality of the canned fruit is maturity at harvest. Previous research on fresh peaches showed that flesh firmness, skin ground color, and flesh color were good maturity indices (Rood 1957). Flesh firmness as measured by penetrometer is a destructive test and, hence, is not used for grading fresh market peaches. Ground color is used for fresh peach maturity assessment in California and South Carolina (Delwiche and Baumgardner 1985). Because the flesh is exposed after canning, flesh color is used for maturity evaluation of fresh clingstone peaches in California.

Present California state grade regulations require the use of color standards in the form of plastic disks for maturity evaluation. The color disks are intended

Journal of Food Process Engineering 10 (1989) 269-284.

to match the minimum flesh color of peaches necessary to insure a canned product "choice" grade (USDA grade B). Maturity evaluations are conducted by inspection personnel at field grade stations on random samples of peaches from the harvest bins. One of 3 color disks is selected by the processor to be used as the grade standard. Comparisons are made between the color disks and flesh exposed after removal of a 6.4 mm thick slice from the smaller cheek. Problems have arisen because these color disks are difficult to use and do not insure adequate color and uniformity of color after processing. Several factors contribute to these problems: (1) the color of the disks do not match the actual peach flesh color at the appropriate stage of maturity, (2) flesh color varies as a function of cut surface position, and (3) the difficulty of using a single color standard rather than a gradient of colors corresponding to immature through mature fruit.

In previous research, fresh clingstone peaches were separated into groups based on colorimeter measurement and the canned halves were graded by sensory panel (Fuleki and Cook 1975). Hunter color coordinates (L, a, and b) of the fresh and canned flesh from 2 cultivars were compared. The results showed a strong relationship between the "a" value (i.e., the red-green color coordinate) of the fresh flesh and quality of the canned product. Kader *et al.* (1982) also reported that canned flesh color can be predicted from fresh flesh "a" values (using Gardner Rd, a, and b coordinates).

Research began at the University of California at Davis several years ago to relate the optical properties of clingstone peaches to maturity. Color was measured as a function of cultivar, maturity, and flesh position using a tristimulus colorimeter. The potential for automatic color sorting of whole fruits and peeled halves was evaluated by measurement of spectral characteristics with a spectrophotometer (Delwiche *et al.* 1987). Based on this work, a trial color chart for maturity evaluation was developed and tested during the 1987 season. The results of this work are summarized herein.

The specific objectives of this research were: (1) to determine the relationship between fresh flesh color matched with the trial maturity chart and canned color; and (2) to measure the progression of flesh color as a function of time during fruit growth and maturation; and (3) to develop final specifications for a new clingstone peach maturity chart.

EXPERIMENTAL METHODS

Fruit Handling

Samples of 5 peach cultivars spanning the harvest season were collected from commercial orchard blocks in Yuba City, California. For the canning study (objective 1), approximately 300 peaches of varying maturity were hand-picked

and placed in cold storage at 0°C. On the afternoon before canning, the peaches were removed from the cooler and visually separated into 3 flesh color classes (1A, 4A, and 7A) by comparison with the trial color chart. These separations were made under standard grading lights (5500–6000 °K) by removing a 6.4 mm thick slice from 1 cheek of each peach with the standard grading knife. After the color comparisons, flesh firmness was measured on the sliced cheek using a penetrometer (Model UC Fruit Firmness Tester, Western Industrial Supply, San Francisco, California, USA) with a 7.9 mm diameter tip. The segregated peaches were immediately put back in cold storage. On the following morning, 60 fruit from each color class were canned and 20 fruit were measured for fresh color. Color changes between harvest and canning were assumed negligible due to the low storage temperature.

For the time-progression study (objective 2), 4 trees near the center of each orchard block were marked. Ten "typical" fruit were picked from each tree and the combined 40 peach sample was immediately brought to the lab for color measurement. This sampling procedure was repeated 5 times for each cultivar, starting approximately 2 weeks before the expected harvest date and continuing about a week beyond the first commercial harvest.

Canning

The peaches were mechanically halved and pitted, peeled in a 1.25% lye bath, and rinsed with water. The sliced and punched halves were discarded. No. 2 1/2 cans were hand-packed with about 0.54 kg of fruit and filled with about 0.31 kg of 30° Brix syrup (containing approximately equal parts of sucrose, corn syrup, and high-fructose corn syrup). The cans were vacuum sealed at 50 kPa, sterilized in a rotary cooker at 100°C for 20 min, and stored at room temperature. Tests of the canned flesh color were conducted after 5–6 months storage.

Color Measurement

Color was measured by tristimulus colorimeter (Model D25A-PC2, Hunterlab, Reston, Virginia, USA) using 45° incident dual beam illumination on the sample plane and a 0° viewing angle. The colorimeter was standardized with the yellow calibration plate ($X = 61.1$, $Y = 61.6$, $Z = 43.0$, CIE standard illuminant C, CIE 1931 standard observer). All color data are reported in CIELAB (i.e., L*, a*, and b*) color coordinates according to the ASTM recommendation (Standard E308-85).

Spectral characteristics were measured by spectrophotometer (Model 330, Perkin-Elmer, Norwalk, Connecticut, USA) to check the colorimeter readings. The spectrophotometer used a 60 mm diameter integrating sphere, 18 mm diameter viewing aperture, 0° illumination, and 90° viewing angle. Diffuse reflectance was measured from 360 to 780 nm in 10 nm increments and converted

to tristimulus values using weighted-ordinate integration (ASTM Standard E308-85).

Significant problems were found in the early phase of this research with luminance distortion caused by the small aperture of the colorimeter (12.7 mm) and the low light scattering (i.e., translucency) of peach tissue (Delwiche *et al.* 1987). To reduce these effects, the colorimeter was configured with a 25.4 mm aperture and the light magnification lenses in place. The result was a highly illuminated spot in the center of the sample plane and a halo of light around the spot caused by diffuse body reflection (Hunter 1975). Preliminary tests were made on 10 peaches (cultivar Starn) comparing these 2 colorimeter configurations with the standard configuration (50.8 mm aperture, no lenses) and the spectrophotometer. The results (Table 1) showed that colorimeter readings with the 25.4 mm aperture were in reasonable agreement with those from the 50.8 mm aperture and the spectrophotometer. Luminance distortion was clearly evident with the small colorimeter aperture.

Instrument color measurements of the fresh peaches were made on the flesh immediately below the skin (exposed using a potato peeler) and flesh at the standard grading cut (exposed using the grading knife). Measurements of the canned peach halves were made on the convex side covered with syrup.

Visual measurements of fresh flesh color for the canning study were made with the trial maturity chart. The chart was constructed of 7 sections of lacquer covered paper with a mat finish and laminated in clear plastic. A 19 mm hole was punched on the border between adjacent colors to permit comparison of the peach flesh with 2 colors. Based on data collected during 1986, the colors were

TABLE 1.
COMPARISON OF COLOR MEASUREMENT CONFIGURATIONS ON STARN PEACH FLESH†

	L*	a*	b*	x	y
Colorimeter					
12.7 mm aperture + lenses	68.4 d	7.3 b	62.7 c	0.460 c	0.442 b
25.4 mm aperture + lenses	75.0 b	11.4 a	72.2 ab	0.474 ab	0.443 b
50.8 mm aperture	76.7 a	10.9 a	70.5 b	0.468 b	0.440 b
Spectrophotometer					
18 mm aperture	72.4 c	9.9 a	72.6 a	0.475 a	0.448 a

†Sample size = 10 fruit. Means with same letter are not significantly different by Duncan's multiple range test, $\alpha = 0.05$.

TABLE 2.
COLORIMETER MEASUREMENTS OF 1987 TRIAL COLOR CHART†

Color #	L*	a*	b*
1A	77.2	-1.6	65.2
2A	77.5	0.4	65.6
3A	77.2	2.7	67.0
4A	77.4	4.3	64.5
5A	77.9	6.6	64.6
6A	77.8	8.7	66.5
7A	77.6	10.5	66.4

†Measurements on laminated color chart with 25.4 mm aperture and yellow tile standardization.

specified with constant L* and b* values (77.2 and 62.8, respectively) and a 2 unit increment of a* value (-2.0 to 10.0). Actual color measurements of the chart are given in Table 2.

Visual measurements of canned flesh color were made under indirect daylight with the USDA color standards for canned clingstone peaches. Colorimeter measurements of these standards are shown in Table 3.

RESULTS AND DISCUSSION

Average fresh flesh colors for the canning study are shown in Table 4 by cultivar and color class. Peaches separated into the 3 color classes by the grader showed about the same L* (luminance coordinate) readings and a steady increase

TABLE 3.
COLORIMETER MEASUREMENTS OF THE USDA COLOR STANDARDS FOR CANNED CLINGSTONE PEACHES†

USDA Color Model	Grade	L*	a*	b*
CLC	C	68.4	3.6	70.7
CLB	B	71.2	4.2	73.4
CLA	A	66.0	9.9	74.1

†Average of 4 measurements with 25.4 mm aperture and yellow tile standardization.

TABLE 4.
COLOR AND FIRMNESS OF FRESH FLESH AT THE STANDARD GRADING CUT†

Cultivar	Color Class	L*	a*	b*	Firmness
					N
Carson					
	1A	72.3 (1.8)	3.9 (2.1)	70.4 (2.2)	52.0 (5.5)
	4A	74.5 (1.3)	12.2 (2.8)	74.4 (1.7)	42.3 (5.8)
	7A	74.3 (0.9)	15.4 (1.8)	74.1 (2.4)	33.4 (4.5)
Andross					
	1A	74.4 (2.2)	4.4 (3.0)	72.1 (2.3)	46.7 (5.6)
	4A	76.1 (1.4)	8.9 (2.3)	75.9 (2.4)	34.3 (5.5)
	7A	76.2 (1.1)	13.6 (2.0)	76.9 (2.8)	23.1 (3.8)
Halford					
	1A	75.6 (1.5)	3.9 (3.9)	66.9 (1.9)	41.8 (6.6)
	4A	76.3 (1.8)	9.5 (3.3)	69.7 (2.2)	31.6 (5.4)
	7A	75.0 (1.7)	15.7 (3.0)	70.2 (2.7)	30.2 (6.9)
Dr. Davis					
	1A	77.9 (1.5)	1.1 (2.2)	63.7 (4.2)	52.9 (6.4)
	4A	77.2 (1.0)	12.8 (2.1)	71.1 (1.5)	41.8 (7.2)
	7A	75.4 (1.2)	17.6 (2.5)	69.0 (2.6)	29.4 (4.8)
Starn					
	1A	76.5 (1.3)	4.5 (2.8)	66.8 (3.3)	47.6 (6.7)
	4A	76.0 (1.2)	9.1 (2.5)	70.2 (2.0)	34.7 (6.7)
	7A	76.2 (1.2)	10.8 (1.4)	67.8 (4.1)	27.1 (7.6)
(Combined)					
	1A	75.3 (2.5)	3.6 (3.1)	68.0 (4.1)	48.2
	4A	76.0 (1.6)	10.5 (3.1)	72.3 (3.1)	36.9
	7A	75.4 (1.4)	14.6 (3.1)	71.6 (4.5)	28.6

†Sample size = 20 fruit/color class for colorimeter measurements and 60 for firmness. Standard deviations shown in parentheses.

in a* (green/red chrominance coordinate) from class 1A to 7A. In general, the measurements of b* (blue/yellow chrominance coordinate) were slightly lower for color class 1A than 4A and 7A, although the magnitude of these differences was not as large as for a*. The overall visual interpretation of these data indicates a shift from yellow-green to yellow-red (i.e., orange) flesh coloration, with approximately constant lightness.

Increased maturity of peaches in the higher color classes is further evidenced by the steady decrease in flesh firmness from color class 1A to 7A. Average firmness measurements were 48.2, 36.9, and 28.6 N, respectively. The low firmness at higher flesh color levels could cause unacceptable losses due to bruising, mispitting, or over-peeling. Furthermore, the relationship between color and flesh firmness varies due to factors such as soil type, cultural practice, climate, weather, etc. Therefore, a new maturity chart must cover a sufficient range of color to allow for local adjustments due to these effects.

The average flesh color readings in Table 4 were compared with the color chart measurements in Table 2 to determine the accuracy of segregation by the

grader. The visual difference between adjacent colors on the chart was small ($\Delta E \approx 2$) and caused the grader difficulty when making such distinctions. Therefore, the grader placed peaches with flesh matching colors 1A and 2A in color class 1A, 3A to 5A in color class 4A, and 6A to beyond 7A in color class 7A. The data in Table 4 compared with the color chart measurements in Table 2 show that the grader tended to under-estimate a* for color classes 1A and 4A. Part of this discrepancy may have been due to the difference in b* values between the maturity chart and the actual peaches.

Color measurements of the canned flesh and the USDA color grade are shown by cultivar and color class in Table 5. Compared with the fresh peaches, the canned fruit had roughly similar chrominance but lower luminance by about 15 L* units. This suggests that the primary change due to canning was a breakdown in cell structure causing a decrease in light scattering and, hence, an increase in flesh translucency. Color class 1A was graded USDA grade C for all cultivars, whereas color classes 4A and 7A were all rated grade A. None of the canned peach samples were judged to match color model B. Theoretical color matches (shown on the right in Table 5) were calculated by determining the minimum

TABLE 5.
COLOR AND USDA COLOR GRADE OF THE CANNED FLESH†

Cultivar	Color Class	L*	a*	b*	USDA Color Grade Visual	USDA Color Grade Theoretical
Carson						
	1A	56.8 (1.7)	4.2 (1.1)	67.3 (2.2)	C	C
	4A	58.4 (1.6)	5.1 (1.3)	63.2 (1.8)	A	C
	7A	59.2 (1.8)	6.0 (1.5)	65.4 (1.7)	A	C
Andross						
	1A	61.4 (2.3)	4.0 (1.8)	65.7 (2.5)	C	C
	4A	63.8 (1.5)	7.7 (1.8)	70.9 (3.1)	A	A
	7A	63.2 (2.3)	9.3 (2.2)	71.7 (3.3)	A	A
Halford						
	1A	59.9 (2.2)	3.4 (1.7)	60.5 (3.1)	C	C
	4A	60.7 (1.8)	7.9 (2.6)	66.2 (2.5)	A	A
	7A	60.9 (1.6)	11.1 (2.4)	68.5 (2.9)	A	A
Dr. Davis						
	1A	56.2 (1.8)	1.7 (1.1)	61.0 (2.7)	C	C
	4A	57.2 (1.7)	7.0 (2.1)	66.0 (2.7)	A	A
	7A	58.2 (2.0)	11.3 (2.8)	67.8 (2.7)	A	A
Starn						
	1A	56.9 (1.9)	2.2 (1.3)	61.3 (2.6)	C	C
	4A	58.7 (1.5)	7.2 (3.0)	63.8 (3.5)	A	C
	7A	59.1 (1.6)	7.4 (2.7)	65.8 (3.0)	A	A
(Combined)						
	1A	58.4 (2.9)	3.2 (1.8)	63.3 (3.9)		C
	4A	60.0 (2.9)	6.9 (2.4)	66.3 (3.9)		C
	7A	60.3 (2.6)	8.9 (3.1)	67.9 (3.6)		A

†Sample size = 20 fruit/color class. Standard deviations shown in parentheses. Theoretical color grade based on minimum distance to color model data.

Euclidean distance in color space (i.e., ΔE) between the average canned flesh values and the color standards (Table 3). For several of the cultivars, the theoretical color match differed from the visual grade (which illustrates the difficulty in quantifying visual perceptions of nonopaque biological materials). The discrepancies were primarily due to the difference in b* value between the color models and the flesh which distorted the effects due to a* differences. The lack of visual or theoretical color matches with color model B was caused by its higher luminance.

Processors have reported that for some cultivars, flesh exposed by the standard grading knife is different in color from flesh closer to the skin. This would complicate the task of fresh grading to insure canned color grade since the canned evaluation is on flesh just below the skin. Previous results showed significant color differences between the 2 measurement locations (Delwiche *et al.* 1987). Average colorimeter readings of the surface flesh are shown in Table 6. Compared

TABLE 6.
COLOR OF FRESH FLESH AT THE PEACH SURFACE†

Cultivar	Color Class	L*	a*	b*
Carson				
	1A	77.1 (1.5)	2.4 (3.3)	64.2 (3.6)
	4A	78.6 (1.4)	8.7 (2.6)	65.1 (3.3)
	7A	78.9 (1.1)	11.5 (1.8)	65.8 (2.7)
Andross				
	1A	78.4 (2.1)	3.7 (2.3)	65.2 (3.4)
	4A	79.4 (1.2)	7.4 (2.6)	68.8 (3.4)
	7A	79.5 (3.4)	10.8 (3.4)	67.9 (3.6)
Halford				
	1A	79.7 (1.7)	-1.8 (3.6)	57.6 (2.4)
	4A	80.1 (1.6)	7.1 (4.4)	64.4 (3.3)
	7A	78.7 (2.2)	13.2 (3.5)	64.5 (3.6)
Dr. Davis				
	1A	79.6 (1.8)	0.4 (2.4)	62.5 (2.9)
	4A	79.7 (1.4)	12.7 (2.5)	65.7 (3.5)
	7A	77.8 (1.6)	17.5 (2.8)	63.4 (2.7)
Starn				
	1A	79.1 (1.3)	1.9 (3.5)	60.6 (3.2)
	4A	79.2 (1.5)	6.6 (3.5)	63.5 (3.4)
	7A	79.9 (1.2)	8.8 (1.6)	64.0 (3.9)
(Combined)	1A	78.8 (1.9)	1.3 (3.6)	62.0 (4.1)
	4A	79.4 (1.5)	8.5 (3.8)	65.5 (3.8)
	7A	79.0 (1.7)	12.4 (3.8)	65.1 (3.7)

†Sample size = 20 fruit/color class. Standard deviations shown in parentheses.

with flesh at the standard grading cut, the surface flesh was lighter by 3–4 L* units, greener by about 2 a* units, and less yellow by about 6 b* units.

Data from the time-progression study were used to determine the rate of flesh color change during fruit growth and maturation. To enable comparison among cultivars, the variable time was normalized by calculating the number of days from first commercial harvest to the sample time (negative values correspond to time before harvest). Average flesh color at the standard cut surface is plotted by cultivar in Fig. 1–3. Several observations are consistent with the canning study data in Table 4. The plot of L* over time (Fig. 1) showed that the luminance of the peach flesh was relatively constant, particularly for the final week before harvest. In contrast, the value of a* (Fig. 2) steadily increased during the 2 weeks before harvest and, to a lesser degree, after harvest. Color coordinate b* (Fig. 3) showed a slight tendency to increase before harvest, with the exception of the Dr. Davis cultivar. For this cultivar, table 4 and Figure 3 show a large increase in b* value immediately before the onset of horticultural maturity (Watada *et al.* 1984). Both L* and b* curves showed a slight tendency to decline after harvest.

Revision of the trial maturity chart was based on information from the canning study and the time-progression study. Several assumptions were made in the derivation of final specifications:

(1) The canning study showed that fruit selected to match color 4A of the trial chart were all graded USDA color grade A. Therefore, $a^* = 4.0$ was selected as the midpoint of a 7 color sequence.
(2) Field experience showed that the small difference between adjacent colors of the trial chart made grading difficult. Therefore, $\Delta a^* = 3.0$ was selected to give a larger color step and wider maturity range.
(3) The time-progression study showed approximately constant flesh luminance before harvest. Therefore, the maturity chart luminance was fixed at $L^* = 76.5$, corresponding to the average of the first 4 samples.
(4) The time-progression study also showed increasing a* and b* values before harvest. Therefore, data from samples 1–4 were pooled and used to calculate prediction equations for a* and b* as functions of time (Table 7). Linear equations were used in order to maintain a constant color increment for a fixed time step between adjacent colors. Although the data for b* (Fig. 3) appeared quadratic, the linear approximation was judged reasonable for negative time (i.e., the period of greatest interest).

Based on these assumptions, final maturity chart specifications are given in Table 8 (CIE standard illuminant C and 1931 standard observer). The difference between adjacent colors was fixed at 3.2 CIELAB units, corresponding to an approximate time interval of 3.5 days. The color trajectory defined by these

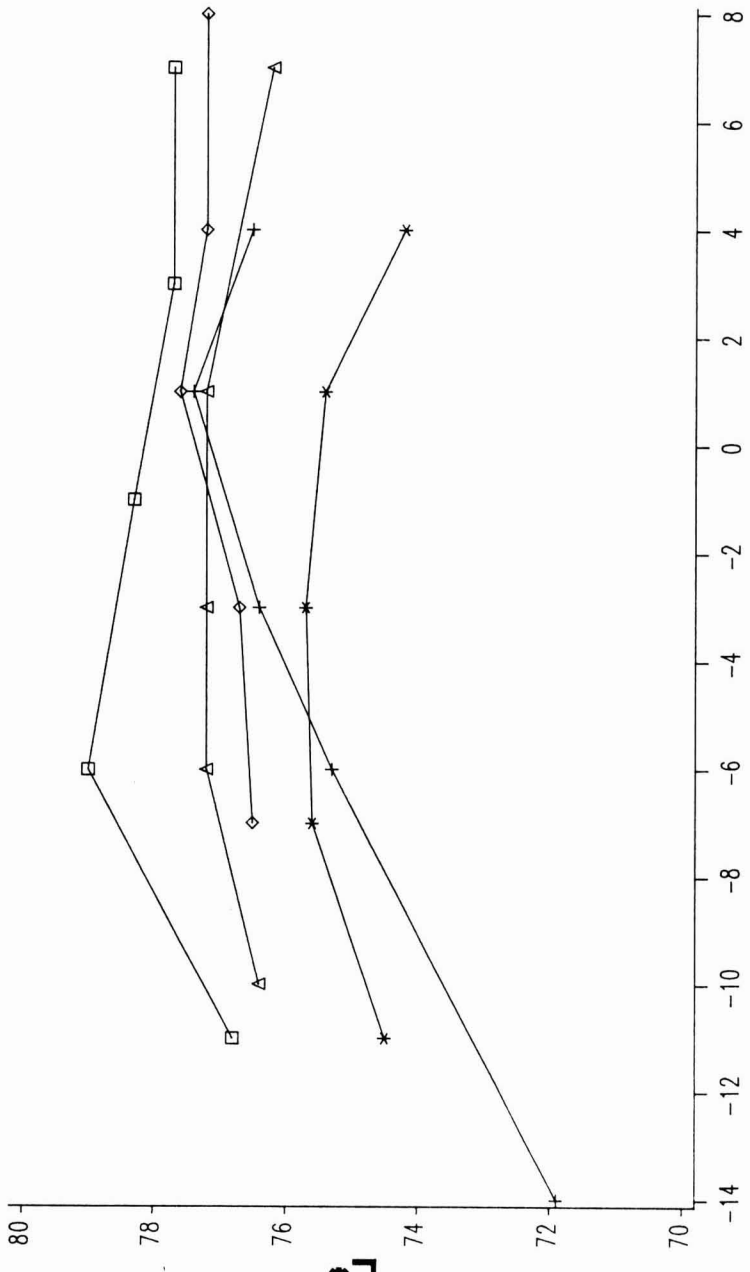

FIG. 1. AVERAGE L* OF THE CUT FLESH VERSUS TIME BEFORE AND AFTER FIRST COMMERCIAL HARVEST

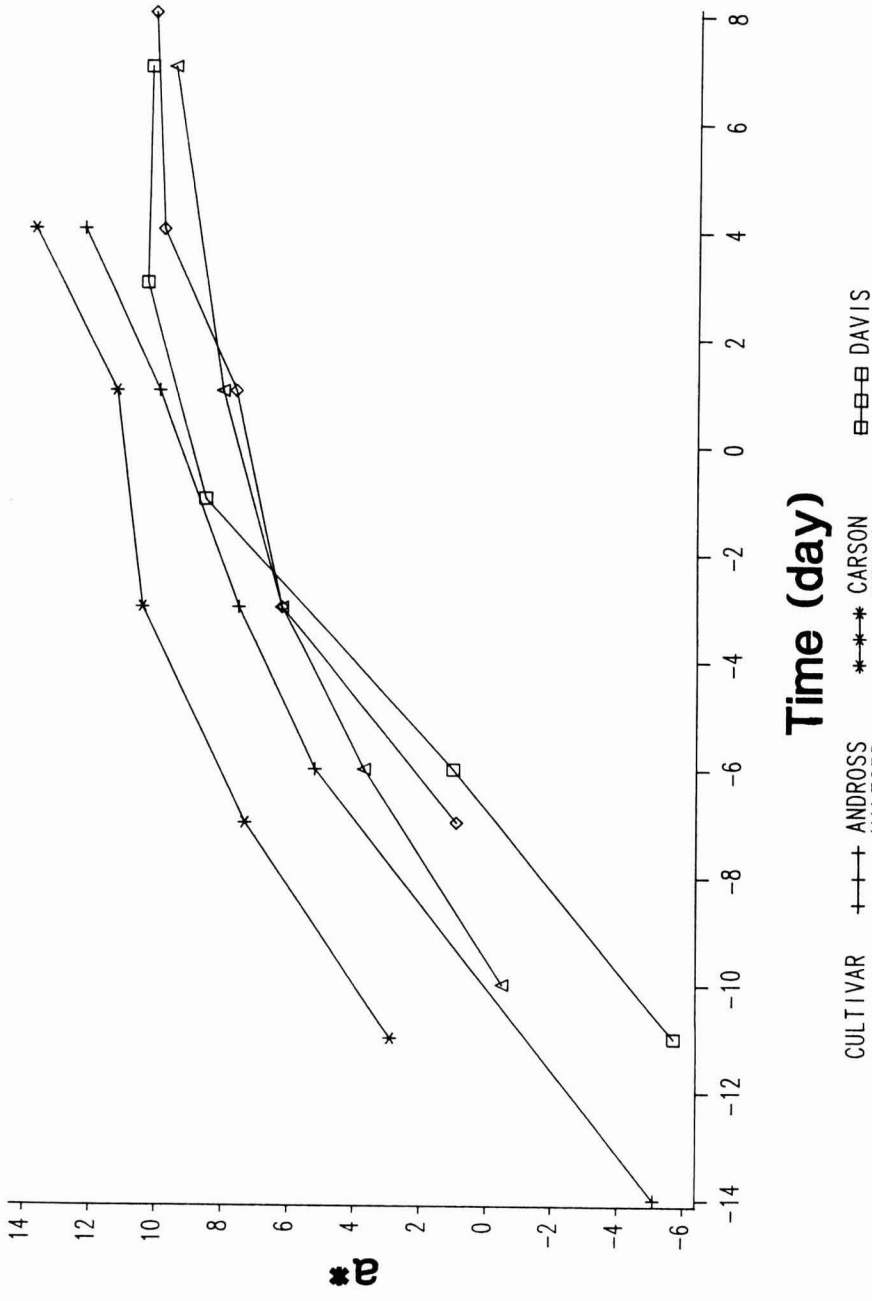

FIG. 2. AVERAGE a* OF THE CUT FLESH VERSUS TIME BEFORE AND AFTER FIRST COMMERCIAL HARVEST

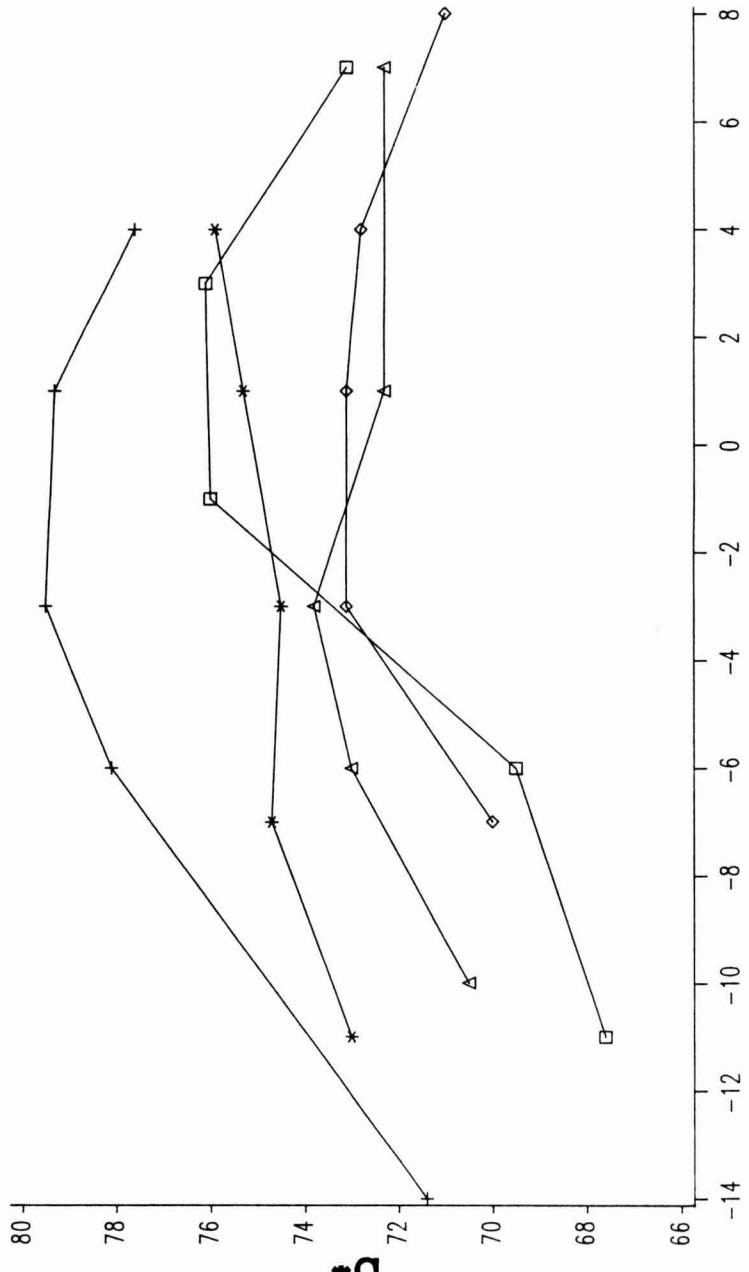

FIG. 3. AVERAGE b* OF THE CUT FLESH VERSUS TIME BEFORE AND AFTER FIRST COMMERCIAL HARVEST

TABLE 7.
LEAST-SQUARES LINEAR EQUATIONS FOR a* AND b* AS FUNCTIONS OF TIME

Dependent Variable	Slope (SE) day^{-1}	Intercept (SE)
a*	0.86 (0.11)††	8.69 (0.71)††
b*	0.30 (0.13)†	74.88 (0.81)††

†, ††Significantly non-zero at the 5% and 1% levels, respectively.

specifications is plotted in the a*-b* color plane shown in Fig. 4. Color number 1 appears green-yellow and corresponds to immature fruit. The point of threshold maturity (corresponding to the onset of horticultural maturity) on the chart will be variable, depending on cultivar, season, and processor, although it will likely fall in the range of color numbers 3–5. Color number 7 appears yellow-orange and corresponds to peaches beyond the point of threshold maturity. Note also that these specifications are for flesh color after removal of a 6.4 mm thick slice from the cheek (the present grading procedure). Increased L* values and decreased b* values would be necessary for flesh nearer the skin.

Color charts based on the specifications given in Table 8 are now being evaluated by the California Cling Peach Advisory Board.

TABLE 8.
FINAL SPECIFICATIONS FOR THE CLINGSTONE PEACH MATURITY CHART†

Color	L*	a*	b*
1	76.5	-5.0	70.1
2	76.5	-2.0	71.2
3	76.5	1.0	72.2
4	76.5	4.0	73.3
5	76.5	7.0	74.3
6	76.5	10.0	75.4
7	76.5	13.0	76.4

†For color evaluation of fresh flesh exposed by the standard grading knife.

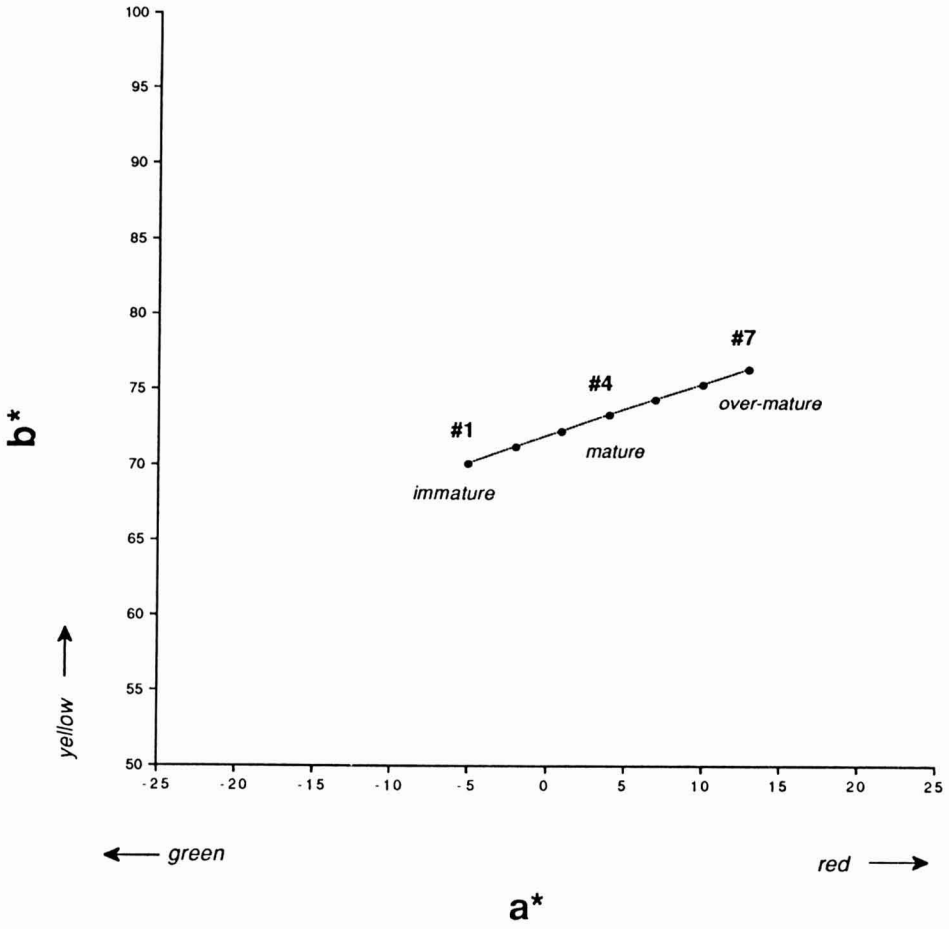

FIG. 4. FINAL MATURITY CHART SPECIFICATIONS PLOTTED IN THE a*–b* COLOR PLANE (L* = 76.5)

CONCLUSIONS

The flesh color of processing clingstone peaches was measured by tristimulus colorimeter (in CIELAB color coordinates) and human grader to provide basic information for development of an improved maturity chart. Peaches from 5 cultivars separated into color classes 4A and 7A with a trial maturity chart (specifications given in Table 2) were all graded USDA color grade A after canning. Fruit in color class 1A were graded USDA color grade C. No canned fruit were judged USDA color grade B due to the higher luminance of color model B compared with A and C. Large differences were found between all of the USDA color models and the actual canned peach flesh.

Over a 2 week period around harvest, fresh flesh L* values (luminance coordinate) were approximately constant, a* values (green/red coordinate) increased steadily before and after harvest, and b* values (blue/yellow coordinate) increased before and decreased slightly after harvest. Linear prediction equations were computed from these data to revise the trial color chart. Final specifications for a new maturity chart were 7 colors of constant luminance (L* = 76.5), linearly increasing a* values (-5.0, to 13.0), and linearly increasing b* values (70.1 to 76.4). The color difference between successive steps, $\Delta E = 3.2$, corresponded to a time increment of 3.5 days. The midpoint of this chart was selected to approximately match color 4A of the trial chart, which yielded USDA grade A canned fruit.

NOMENCLATURE

X, Y, Z $\overset{\Delta}{=}$ CIE tristimulus values using standard illuminant C and the 1931 standard observer functions.

L*, a*, b* $\overset{\Delta}{=}$ CIELAB uniform color scale:

$$L^* = 116\,(Y/100)^{\frac{1}{3}} - 16$$

$$a^* = 500\,[(X/98.041)^{\frac{1}{3}} - (Y/100)^{\frac{1}{3}}]$$

$$b^* = 200\,[(Y/100)^{\frac{1}{3}} - (Z/118.103)^{\frac{1}{3}}]$$

x, y $\overset{\Delta}{=}$ Chromaticity coordinates:

$$x = X/(X + Y + Z)$$

$$y = Y/(X + Y + Z)$$

ΔE $\overset{\Delta}{=}$ Color difference between points i and j in CIELAB color space:

$$\Delta E = [(L^*_i - L^*_j)^2 + (a^*_i - a^*_j)^2 + (b^*_i - b^*_j)^2]^{\frac{1}{2}}$$

ACKNOWLEDGMENTS

Appreciation is expressed for the financial assistance of the California Cling Peach Advisory Board to conduct this research. I also express my appreciation to Scott Mahan, Susan Briggs, and Robert Fenton for help with the laboratory work and data analysis.

REFERENCES

A.S.T.M. 1987 Annual Book of Standards. Section 14, Standard E308-85, 244–291. Amer. Soc. for Testing and Materials, Philadelphia, PA.

DELWICHE, M. J. and BAUMGARDNER, R. A. 1985. Ground color as a peach maturity index. J. Amer. Soc. Hort. Sci. *110*(1), 53–57.

DELWICHE, M. J., TANG, S. and RUMSEY, J. W. 1987. Color and optical properties of clingstone peaches related to maturity. Trans. Amer. Soc. Agr. Eng. *30*(6), 1873–1879.

FULEKI, T. and COOK, F. I. 1975. Relationship of maturity as indicated by flesh color to quality of canned clingstone peaches. Can. Inst. Food Sci. Technol. J. *8*(4), 43–46.

HUNTER, R. S. 1975. *The Measurement of Appearance,* Ch. 16, John Wiley & Sons, New York.

KADER, A. A., HEINTZ, C. M. and CHORDAS, A. 1982. Postharvest quality of fresh and canned clingstone peaches as influenced by genotype and maturity at harvest. J. Amer. Soc. Hort. Sci. *107*(6), 947–951.

ROOD, P. 1957. Development and evaluation of objective maturity indices for California freestone peaches. Proc. Amer. Soc. Hort. Sci. *70,* 104–112.

WATADA, A. E., HERNER, R. C., KADER, A. A., ROMANI, R. J. and STABY, G. L. 1984. Terminology for the description of developmental stages of horticultural crops. HortSci. *19*(1), 20–21.

STUDIES OF WATER TRANSPORT PHENOMENA DURING POTATO-DRYING

INGRID LAMBERG

Division of Food Engineering, Lund University,
P.O. Box 124, S-221 00 Lund, Sweden

Accepted for Publication September 23, 1988

ABSTRACT

Sorption isotherms and drying mechanisms of Bintje potatoes have been investigated experimentally. The product temperature and the moisture content was determined during the drying experiments.

A simulation method to estimate the diffusion coefficient and the moisture content profiles for the potatoes was performed by means of a finite-difference computer program. Experimentally determined moisture contents were compared with calculated for different estimated values of the diffusion coefficient. If the diffusion coefficient was assumed to be $0.8 \cdot 10^{-9}$ m^2/s *the correlations were acceptable. The simulated moisture content profiles also gave the surface moisture content.*

The surface mass transfer coefficient has been calculated. the resulting β *values were in the range of 0.014–0.029 m/s.*

INTRODUCTION

Potato-drying is one of the operations in the production of French fries, and follows the blanching stage. The reasons for drying the potatoes are to remove surface water and to reduce the water content in order to minimize fat uptake during deep fat frying. To model and optimize the drying stage it is necessary to know the diffusivity (diffusion coefficient) of water in the potatoes.

$$\frac{dX}{dt} = D\frac{d^2X}{dx^2} \tag{1}$$

is used to calculate this coefficient.

Normally D is not constant for food products but a function of the water content. In this case however the range of moisture content investigated is rather

Journal of Food Process Engineering 10 (1989) 285-299.

narrow (4.70 to 2.14 g water/g dry solid). It was therefore convenient to suppose a constant D-value then being an average value within the water content values investigated.

The water transport phenomenon is rather complicated, as the moisture transfer may occur by different mechanisms. Normally, the ''apparent'' diffusion coefficient is measured. Measurements of this apparent diffusion coefficient have been described by many authors. Diffusion has been presented mathematically by Crank (1975). Fish (1958) studied diffusion and thermodynamics of water in potato starch gel. He has also presented work on dried potatoes.

Saravacos and Charm (1962) studied the drying mechanism of potatoes. They also compared the effect on drying rate of blanched and unblanched potato.

Vaccarezza, Lombardi and Chirife (1974) investigated the influence of several variables on the drying rate of sugar beet. Fick's law was used as a mathematical tool and Vaccarezza and Chirife (1975) then proposed a method to predict the diffusivity from drying experiments of sugar beet.

The aim of this study has been to find a reliable simulated model for calculating the D-value and the moisture content profile, compared to applied experiments. From the experiments the surface mass transfer coefficient, β, has also been determined.

MATERIALS AND METHODS

The food substrate was Bintje potatoes supplied by Felix Co., Kävlinge. The moisture contents of the potatoes in the different experiments varied between 4.38 and 4.70 g water/g dry solid, the glucose content was 8.07 g/kg wet basis and fructose content 5.13g/kg wet basis. Glucose and fructose contents were determined enzymatically, (Boehringer Mannheim). A mean value of the density was 1080 kg/m^3.

The blanching procedure took place in a thermostatically controlled water bath, see (Lamberg and Hallström 1986). The drying was performed in a convection oven, (Skjöldebrand 1979) with well controlled air temperature and air velocity. The humidity of the air could be varied by injecting steam.

The product temperature, in this investigation the center temperature, the dry air and wet-bulb temperatures were measured with four Cr/Al thermocouples with a thickness of 0.3 mm. The wet-bulb temperature was measured by means of thermocouples covered with a wick immersed in a beaker containing distilled water. The air velocity was measured with an anemometer.

Sorption isotherms

Sorption isotherms for potatoes were experimentally determined by the saturated-salt solution method (Wolf, Spiess and Jung 1985). The potatoes were

peeled and dipped in 50 mg/kg chlorine solution for 10 s. Cylindrical samples, 20 mm in diameter, were stamped out of the most homogeneous part of the potato, between the hilum and the center. Slices 5 mm thick were then cut from the cylinder.

For adsorption experiments the potato slices were freeze-dried and for desorption the slices were cut and weighed immediately. The equilibrium temperatures were 15 and 60°C during the desorption and during adsorption 15, 40 and 60°C.

Drying

For the drying experiments the potatoes were cut into strips $13 \times 13 \times 50$ mm, Fig. 1.

Six strips were heat equilibrated in a 20°C water bath for 15 min and blanched in a wire net cage, at 75°C for 15 min. Two of the strips were used for dry substance determination and the other four were placed on a wire net tray in the oven. The drying process started 4 min after blanching. Drying was carried out at various temperatures both with dry and humidified air. Product temperature, and dry air and wet-bulb temperatures were recorded in one series and product weight, dry air and wet-bulb in another series. Each series was repeated six times. After each weight series the moisture content of the crumb and a 0.8 mm skin layer was determined, Fig. 1.

The moisture content was determined by an oven-drying method; 70°C for 24 h and 105°C for 1 h. The dehydration conditions studied are presented in Table 1. The air velocity was 3 m/s and the drying time was 15 min.

TABLE 1. DEHYDRATION CONDITIONS

Dry air temp (°C)	Wet air temp (°C)	Relative humidity (%)
60	24	3
60	36	20
60	47	49
80	30	2
80	46	16
80	55	30
80	60	40
99	34	1
99	52	10
99	62	18

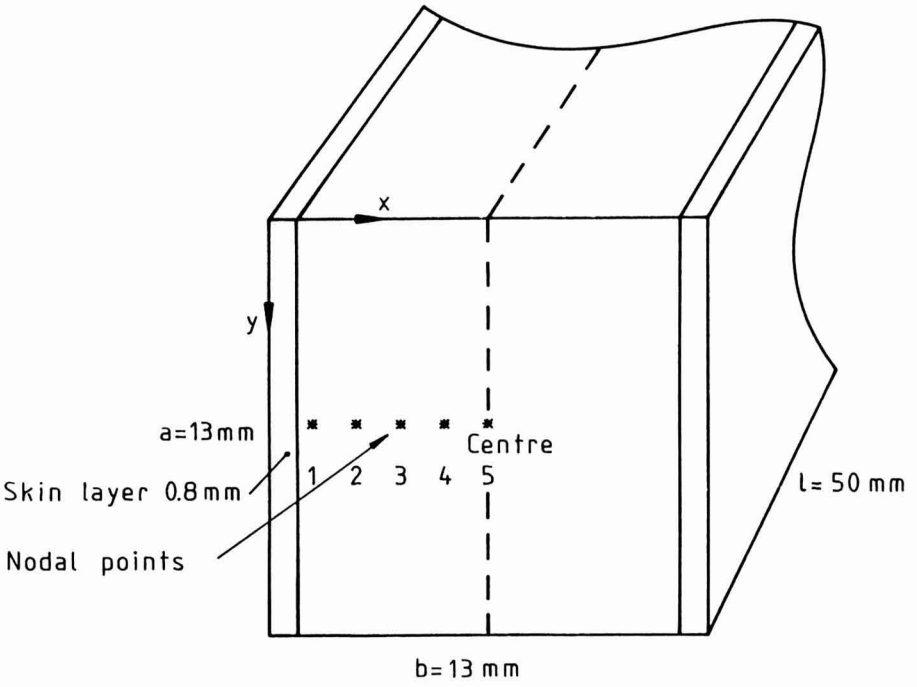

FIG. 1. POTATO MODEL (13 × 13 × 50 mm)

Calculations

The theoretical moisture distribution is calculated using Fick's law

$$\frac{dX}{dt} = D\left(\frac{d^2X}{dx^2} + \frac{d^2X}{dy^2} + \frac{d^2X}{dz^2}\right) \tag{2}$$

To solve the equation, a computer program based on the finite-difference technique is used.

The shape chosen is an infinitely long rectangular rod or strip, see Fig. 1. The other two dimensions are chosen to equal those of the potato strips used in the experiments.

The surface moisture content is determined by means of repeated simulations and is close to the experimental skin layer moisture content, X_s. The initial moisture content, X_o, used is 4.5 g water/g dry solid.

Different diffusion coefficients are used to simulate moisture contents in the rod. Experimental moisture contents then are compared with simulated values and in this way the moisture content profile is determined.

Program inputs used in the model are:
The diffusion coefficient, rod thickness in x- and y-directions, number of space divisions, surface moisture content at different times, initial moisture content and time step.

The mass transfer coefficient, β, is calculated from the Eq. (3).

$$\Delta g = \beta A \, \Delta P \frac{M(H_2O)}{RT} \tag{3}$$

Δg, the water flux resulting from the drying experiments, ΔP, is the pressure difference between the water vapour pressure at the surface at 100% relative humidity and the vapour pressure in the air bulk and A is the total area of four strips. T, the temperature.

RESULTS

Sorption Isotherms

The sorption isotherms are presented in Fig. 2. Both adsorption and desorption curves show a temperature dependency.

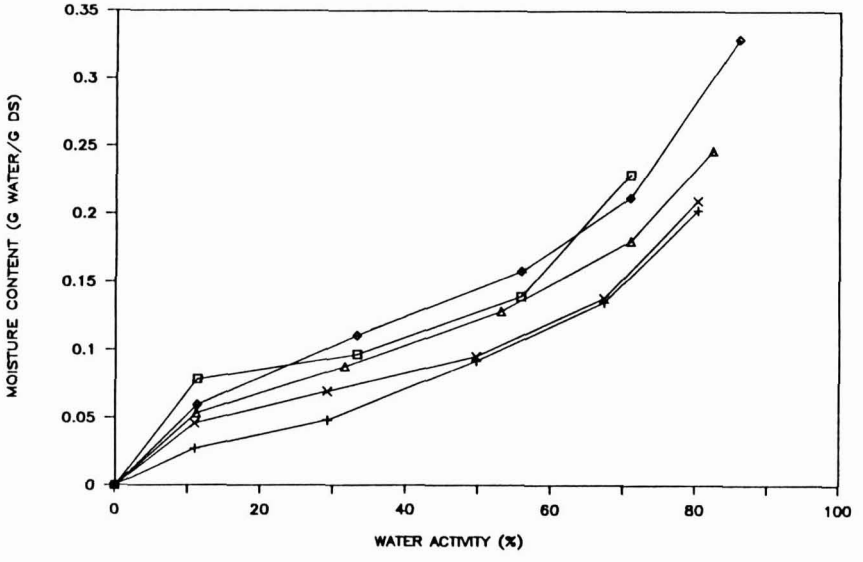

FIG. 2. SORPTION ISOTHERMS OF POTATOES

□ Desorption 15°C
\+ Desorption 60°C
◇ Adsorption 15°C
△ Adsorption 40°C
× Adsorption 60°C

The adsorption curves are almost parallel above 30% water activity. The desorption at 15°C has a plateau between 10 and 40% water activity.

The desorption and adsorption curves at 15°C, cross at 25% and 67% water activity but the two sorption isotherms at 60°C do not cross, but indicate hysteresis.

Drying Rate

After blanching, the product temperature was 75°C. This temperature drops to 45°C before the drying operation is started. The product temperature was measured for each air temperature and humidity combination during the drying process. The product temperatures differed considerably depending on whether the drying took place in dry or humidified air. During drying with dry air the product temperature decreased towards the wet-bulb temperature, without reaching it, and then rose again. When the drying procedure took place with humidified air the product temperature in all cases reached the wet-bulb temperature, Fig. 3.

The drying rate was calculated from the weight reduction and the total dry solids. In the drying experiments with dry air the drying rate decreased rapidly during the first 200 s, for all temperatures, and after that a constant drying rate

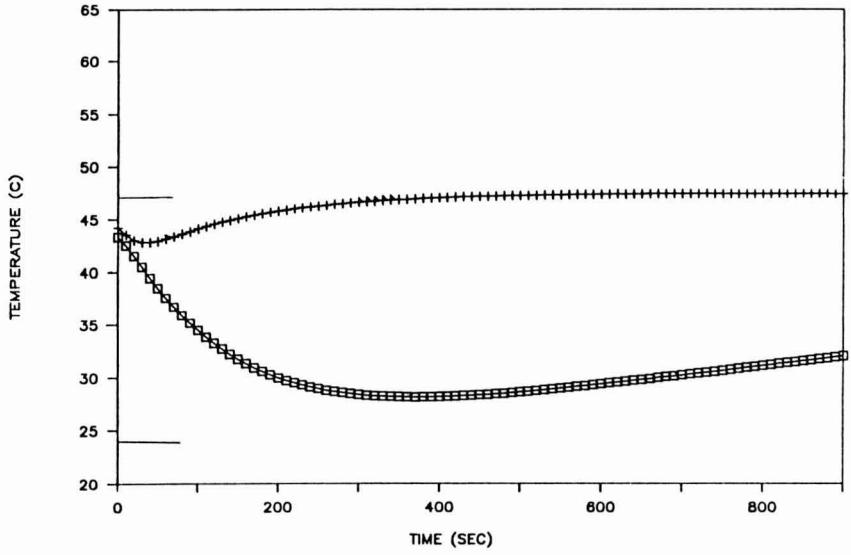

FIG. 3. PRODUCT TEMPERATURE DURING DRYING
□ Dry air 60°C and wet-bulb 24°C, 3% relative humidity
\+ Dry air 60°C and wet-bulb 47°C, 49% relative humidity

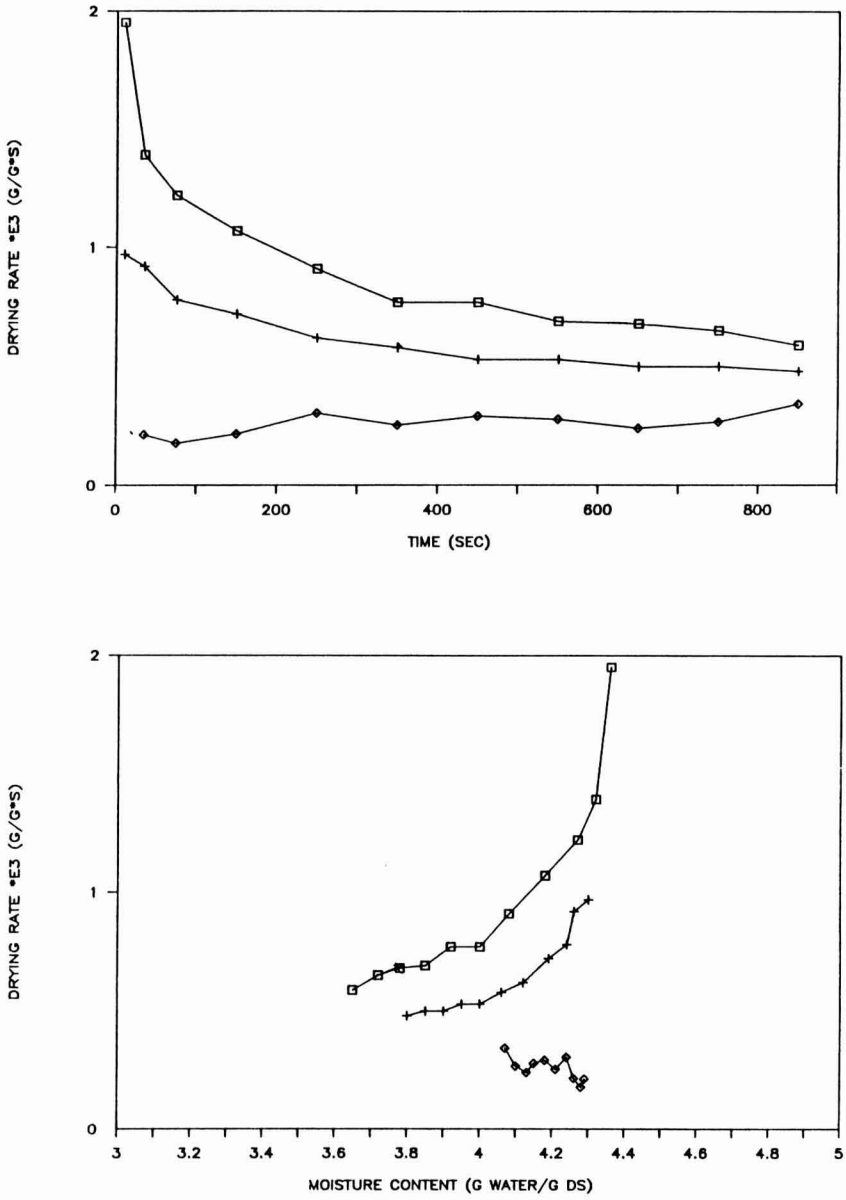

FIG. 4a. DRYING RATE VERSUS TIME AT 60°C

FIG. 4b. DRYING RATE VERSUS MOISTURE CONTENT AT 60°C

□ 3% relative humidity
\+ 20% relative humidity
◇ 49% relative humidity

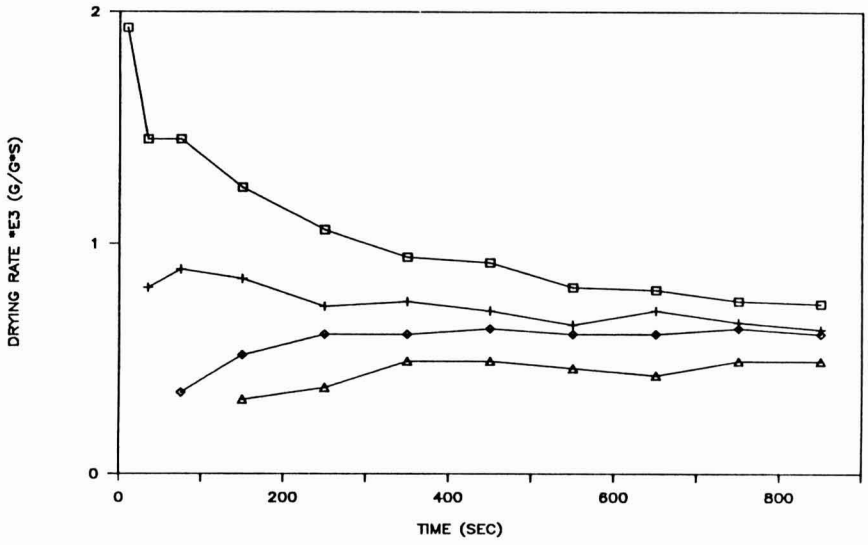

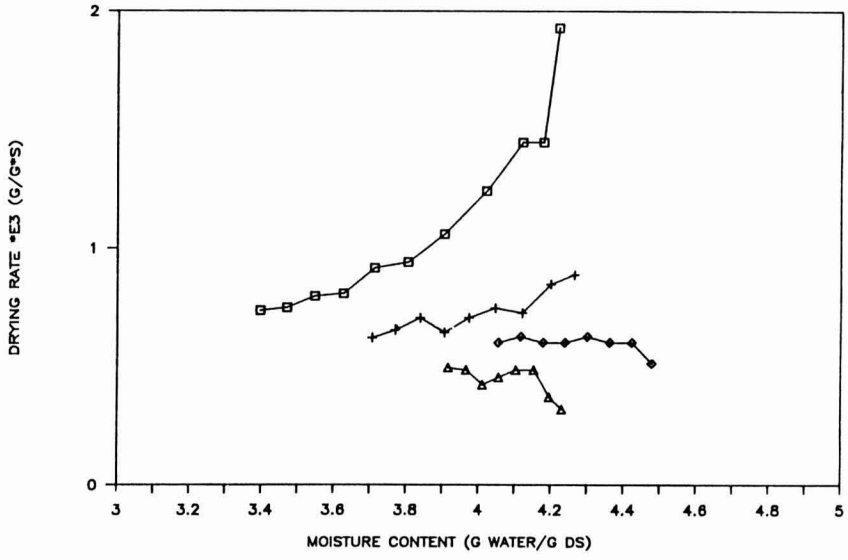

FIG. 5a. DRYING RATE VERSUS TIME AT 80°C

FIG. 5b. DRYING RATE VERSUS MOISTURE CONTENT AT 80°C
□ 2% relative humidity
\+ 16% relative humidity
◇ 30% relative humidity
△ 40% relative humidity

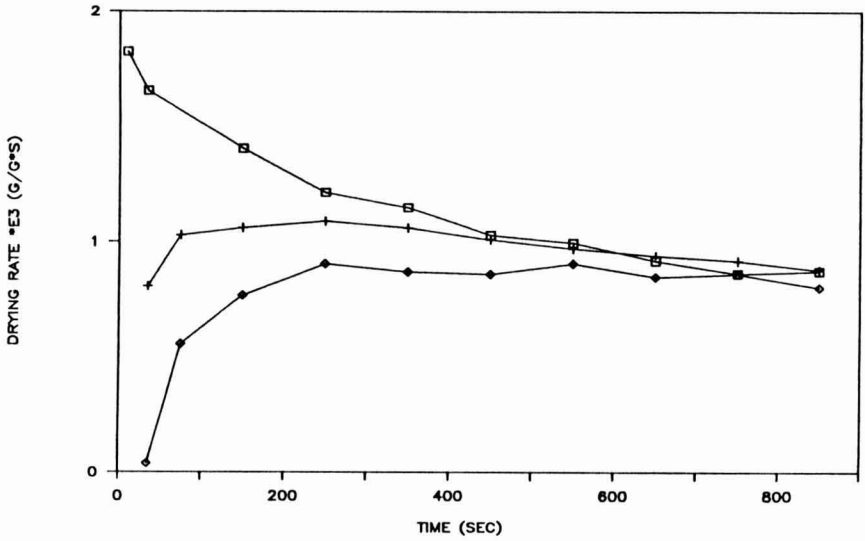

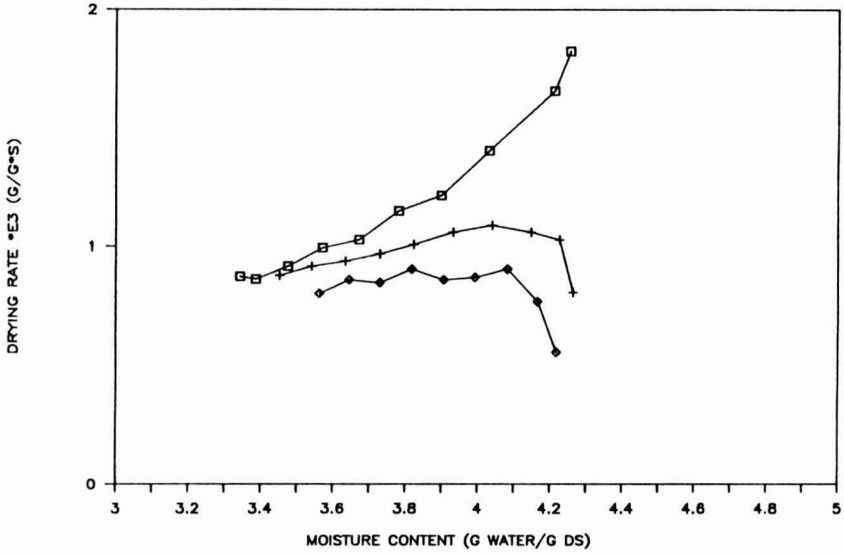

FIG. 6a. DRYING RATE VERSUS TIME AT 99°C

FIG 6b. DRYING RATE VERSUS MOISTURE CONTENT AT 99°C

□ 1% relative humidity
\+ 10% relative humidity
◇ 18% relative humidity

was obtained, Fig. 4a, 5a and 6a. With humidified air the drying rate is almost constant. A tendency towards decreasing drying rate at 60°C and 20% relative humidity was also observed. At 99°C, 10 and 18% relative humidity the drying rate increased at the beginning of the drying procedure. This may be due to condensation.

The figures all represent the mean value of the drying rate for six drying experiments. The drying rate has also been plotted against the moisture content, Fig. 4b, 5b and 6b.

The moisture content during drying decreases as temperature increases. Water is more quickly removed at high temperatures but less quickly with increased humidity. The moisture content decreases with increasing humidity. At 60°C, 3, 20 and 49% relative humidity about 0.75, 0.50 and 0.25 g/g at 80°C, 2, 16, 30 and 40% relative humidity by 0.80, 0.60, 0.45 and 0.35 g/g and finally 99°C, 1, 10 and 18% relative humidity by 0.90, 0.80 and 0.65 g/g respectively. All values are calculated from the drying curves.

Moisture Content Measurements and Calculations

The mean values of the moisture content from the different drying experiments are presented in Table 2. The moisture content varied from potato to potato, due to the variation in natural food materials. The initial moisture content, X_o, reported in this investigation was taken from separate blanched potato pieces.

TABLE 2.
THE INITIAL X_o, FINAL X_f, SKIN LAYER X_s AND CRUMB X_c MOISTURE CONTENTS AT DIFFERENT DRYING TEMPERATURES

Temperature (°C)	Relative humidity (%)	X_o	X_f	X_s	X_c
		(g water/g dry solid)			
60	3	4.54	3.81	2.65	4.55
60	20	4.70	4.22	3.10	4.44
60	49	4.50	4.26	3.85	4.60
80	2	4.45	3.56	2.45	4.48
80	16	4.40	3.71	2.86	4.36
80	30	4.66	4.10	3.27	4.54
80	40	4.41	4.10	3.40	4.40
99	1	4.38	3.54	2.14	4.53
99	10	4.45	3.52	2.40	4.35
99	18	4.50	3.82	2.95	4.59

The values of the initial moisture content, X_o, and the skin layer moisture content, X_s, are used in the finite difference computer program to simulate the moisture content profiles and to determine the diffusion coefficient. Figure 7 represents drying at 60°C. Diffusion coefficient values of $0.8 \cdot 10^{-9}$ m²/s and $8 \cdot 10^{-9}$ m²/s were used in the simulation. The simulation model was an infinitely long rectangular strip, 13mm × 13 mm in cross section.

The mean value of experimentally determined moisture contents of the crust and skin layer were plotted as a function of the nodal points. An initial mean value of 4.5 g water/g dry solid was used for the moisture distribution simulation. The surface moisture content was estimated and in this way determined for each experimental condition. Input values of D were taken from the literature (Saravacos and Charm 1962); (Fish 1957) and then used in the simulation model. $D = 0.8 \cdot 10^{-9}$ m²/s was the value resulting in the best fit to the measured moisture content distribution. A simulation with the surface moisture content equal to the equilibrium moisture content was also performed and the result is presented in Fig. 7.

In Fig. 8 the drying rate versus the air temperature is plotted and summarized for the experiments.

The drying rate in combination with the pressure difference, ΔP, are used to calculate the mass transfer coefficient, β, Eq. (3). The surface temperature is

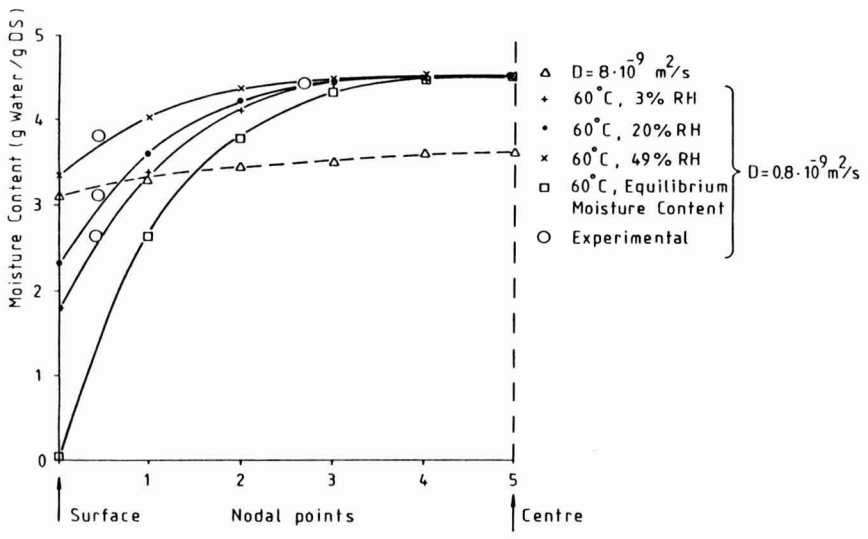

FIG. 7. MOISTURE CONTENT DISTRIBUTION OF THE POTATO AT 60°C (Experimental and simulated).

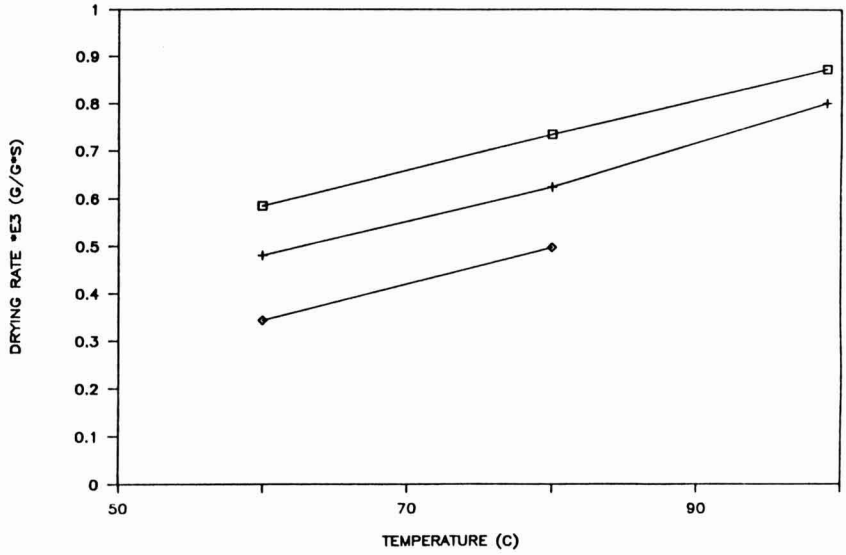

FIG 8. DRYING RATE VERSUS TEMPERATURE
□ 1–3% relative humidity
\+ 16–20% relative humidity
◇ 40–49% relative humidity

approximated, from the temperature measurements, to be the same as the air temperature. The results are presented in Table 3.

TABLE 3.
CALCULATED MASS TRANSFER COEFFICIENTS, β, AT DIFFERENT TEMPERATURES AND HUMIDITY COMBINATIONS

Temperature (°C)	Relative humidity (%)	Mass transfer coefficient (m/s)
60	3	0.016
60	20	0.022
60	49	0.014
80	2	0.016
80	16	0.028
80	30	0.029
99	1	0.017
99	10	0.019
99	18	0.014

DISCUSSION

The sorption isotherms presented in Fig. 2 indicate a temperature dependency, as reported by (Mazza 1982), but for different potato varieties. Some of the adsorption-desorption isotherms seem to show a hysteresis behaviour. However, due to the size of the errors in the measurements this phenomenon may not be significant.

During drying the development of the product temperature shows a dependency on the wet-bulb temperature. Starting from the initial temperature of about 45°C, the product temperature tends to move towards the wet-bulb temperature. This is illustrated in Fig. 3. In one case, the wet-bulb temperature is lower than 45°C while in another case it is a little higher.

After an initial period of 200s, depending on the temperature of the product in relation to the air, it seems that all drying experiments proceeded into a constant-rate period. The falling-rate period is never reached, which is also in accordance with the sorption isotherms, Fig. 2.

(Vaccarezza *et al.* 1974) did not observe a constant-rate period during their drying experiments. The moisture content in their experiments was between 2.5 and 3.6 g water/g solids. The drying experiments performed by (Saravacos and Charm 1962) took place in humidified air and they observed both a constant- and a falling-rate period. The critical moisture content was 3.5g water/g solids.

During the constant rate period it is normally not advisable to use Fick's law in determination of the diffusion coefficient. The reason is of course that during this period the external mass transfer cannot be neglected. However, in this work the moisture content at the surface has not been used in the calculation of D. Instead internal values of the moisture content has been used to deduct a moisture content profile in the material. This profile has then been compared with a similar one according to the Fick's law and calculated by means of computer program based on a finite-difference technique.

In this investigation the D value was $0.8 \cdot 10^{-9}$ m²/s which should be compared with $0.39 \cdot 10^{-9}$ m²/s, at 60°C for potatoes, reported by (Saravacos and Charm 1962). (Vaccarezza *et al.* 1974) found a value of $0.6 \cdot 10^{-9}$ m²/s, at 60°C for sugar beet and (Fish 1957) observed a value of $0.02 \cdot 10^{-9}$, at 25°C for starch. This wide distribution in experimental results is not unusual when measuring D values.

In Fig. 8 the drying rates during the constant rate period from all experiments are summarized. The diagram indicates a behavior dependent on the surface mass transfer coefficient. Accordingly, this coefficient has been calculated using the mass transfer Eq. (3). The drying force ΔP has been calculated as the difference between the water vapor pressure at the surface at 100% relative humidity and the vapor pressure in the air bulk.

The calculations result in β values between 0.014 and 0.029 m/s. Values found in the literature are of the same magnitude (Sjöholm 1986).

ACKNOWLEDGMENTS

This work was supported by the National Swedish Board for Technical Development. The potatoes used were kindly supplied by Felix Co., Kävlinge, Sweden. The author would also like to thank Margareta Johansson for technical assistance.

NOMENCLATURE

A	= area	m^2
β	= mass transfer coefficient	m/s
D	= diffusion coefficient	m^2/s
Δg	= water flux	kg/s
M (H_2O)	= molecule weight, water	g/mol
ΔP	= pressure difference	N/m^2
R	= universal gas constant	J/K·mol
T	= temperature	K
t	= time	s
X	= moisture content	kg/kg
x	= direction coordinate	m
y	= direction coordinate	m
z	= direction coordinate	m

Subscripts

c = crumb
e = equilibrium
f = final
o = initial
s = skin layer

REFERENCES

CRANK, J. 1975. The Mathematics of Diffusion, 2nd ed., Oxford.

FISH, B. P. 1957. Diffusion and equilibrium properties of water in starch. Department of Scientific and Industrial Research. H.M.S.O, London.

LAMBERG, I. and HALLSTRÖM B. 1986. Thermal properties of potatoes and a computer simulation model of a blanching process. J. Food Techn. *21*, 577–585.

MAZZA, G. 1982. Moisture sorption isotherms of potato slices. J. Food Techn. *17*, 47–54.

SARAVACOS, G. D. and CHARM, S. E. 1962. A study of the mechanism of fruit and vegetable dehydration. Food Technol. *1,* 78–81.

SJÖHOLM, I. 1986. Drying of heat sensitive liquids in a thin film. Thesis. Department of Food Engineering, Lund University, Sweden.

SKJÖLDEBRAND, C. 1979. Frying and reheating in a forced convection oven. Thesis. Department of Food Engineering, Lund University, Sweden.

VACCAREZZA, L. M., LOMBARDI, J. L. and CHIRIFE, J. 1974. Kinetics of moisture movement during air drying of sugar beet root. J. Food Techn. *9,* 317–327.

VACCAREZZA, L. M. and CHIRIFE, J. 1975. On the mechanism of moisture transport during air drying of sugar beet root. J. Food Sci. *40,* 1286–1289.

WOLF, W., SPIESS, W.E.L. and JUNG, G. 1985. Standardization of isotherm measurements. (Cost-project 90 and 90 bis). *Properties of Water in Foods.* (D. Simatos and J. L. Mutton, eds.) Dordrecht, Netherlands.

AUTHOR INDEX

Journal of Food Process Engineering *11(1989) 301–302. All Rights Reserved.*

SUBJECT INDEX

Journal of Food Process Engineering *11(1989) 303–304. All Rights Reserved.*

F
N
P

PUBLICATIONS IN FOOD SCIENCE AND NUTRITION

Journals

JOURNAL OF MUSCLE FOODS, N.G. Marriott and G.J. Flick
JOURNAL OF SENSORY STUDIES, M.C. Gacula, Jr.
JOURNAL OF FOOD SERVICE SYSTEMS, O.P. Snyder, Jr.
JOURNAL OF FOOD BIOCHEMISTRY, J.R. Whitaker, N.F. Haard and H. Swaisgood
JOURNAL OF FOOD PROCESS ENGINEERING, D.R. Heldman and R.P. Singh
JOURNAL OF FOOD PROCESSING AND PRESERVATION, D.B. Lund
JOURNAL OF FOOD QUALITY, R.L. Shewfelt
JOURNAL OF FOOD SAFETY, J.D. Rosen and T.J. Montville
JOURNAL OF TEXTURE STUDIES, M.C. Bourne and P. Sherman

Books

CONTROLLED/MODIFIED ATMOSPHERE/VACUUM PACKAGING OF FOODS, A.L. Brody
NUTRITIONAL STATUS ASSESSMENT OF THE INDIVIDUAL, G.E. Livingston
QUALITY ASSURANCE OF FOODS, J.E. Stauffer
THE SCIENCE OF MEAT AND MEAT PRODUCTS, 3RD ED., J.F. Price and B.S. Schweigert
HANDBOOK OF FOOD COLORANT PATENTS, F.J. Francis
ROLE OF CHEMISTRY IN THE QUALITY OF PROCESSED FOODS, O.R. Fennema, W.H. Chang and C.Y. Lii
NEW DIRECTIONS FOR PRODUCT TESTING AND SENSORY ANALYSIS OF FOODS, H.R. Moskowitz
PRODUCT TESTING AND SENSORY EVALUATION OF FOODS, H.R. Moskowitz
ENVIRONMENTAL ASPECTS OF CANCER: ROLE OF MACRO AND MICRO COMPONENTS OF FOODS, E.L. Wynder *et al.*
FOOD PRODUCT DEVELOPMENT IN IMPLEMENTING DIETARY GUIDELINES, G.E. Livingston, R.J. Moshy, and C.M. Chang
SHELF-LIFE DATING OF FOODS, T.P. Labuza
RECENT ADVANCES IN OBESITY RESEARCH, VOL. V, E. Berry, S.H. Blondheim, H.E. Eliahou and E. Shafrir
RECENT ADVANCES IN OBESITY RESEARCH, VOL. IV, J. Hirsch *et al.*
RECENT ADVANCES IN OBESITY RESEARCH, VOL. III, P. Bjorntorp *et al.*
RECENT ADVANCES IN OBESITY RESEARCH, VOL. II, G.A. Bray
RECENT ADVANCES IN OBESITY RESEARCH, VOL. I, A.N. Howard
ANTINUTRIENTS AND NATURAL TOXICANTS IN FOOD, R.L. Ory
UTILIZATION OF PROTEIN RESOURCES, D.W. Stanley *et al.*
FOOD INDUSTRY ENERGY ALTERNATIVES, R.P. Ouellette *et al.*
VITAMIN B_6: METABOLISM AND ROLE IN GROWTH, G.P. Tryfiates
HUMAN NUTRITION, 3RD ED., F.R. Mottram
FOOD POISONING AND FOOD HYGIENE, 4TH ED., B.C. Hobbs *et al.*
POSTHARVEST BIOLOGY AND BIOTECHNOLOGY, H.O. Hultin and M. Milner

Newsletters

FOOD INDUSTRY REPORT, G.C. Melson
FOOD, NUTRITION AND HEALTH, P.A. Lachance and M.C. Fisher
FOOD PACKAGING AND LABELING, S. Sacharow

GUIDE FOR AUTHORS

Typewritten manuscripts in triplicate should be submitted to the editorial office. The typing should be double-spaced throughout with one-inch margins on all sides.

Page one should contain: the title, which should be concise and informative; the complete name(s) of the author(s); affiliation of the author(s); a running title of 40 characters or less; and the name and mail address to whom correspondence should be sent.

Page two should contain an abstract of not more than 150 words. This abstract should be intelligible by itself.

The main text should begin on page three and will ordinarily have the following arrangement:

Introduction: This should be brief and state the reason for the work in relation to the field. It should indicate what new contribution is made by the work described.

Materials and Methods: Enough information should be provided to allow other investigators to repeat the work. Avoid repeating the details of procedures which have already been published elsewhere.

Results: The results should be presented as concisely as possible. Do not use tables *and* figures for presentation of the same data.

Discussion: The discussion section should be used for the interpretation of results. The results should not be repeated.

In some cases it might be desirable to combine results and discussion sections.

References: References should be given in the text by the surname of the authors and the year. *Et al.* should be used in the text when there are more than two authors. All authors should be given in the Reference section. In the Reference section the references should be listed alphabetically. See below for style to be used.

DEWALD, B., DULANEY, J.T., and TOUSTER, O. 1974. Solubilization and polyacrylamide gel electrophoresis of membrane enzymes with detergents. In *Methods in Enzymology,* Vol. xxxii, (S. Fleischer and L. Packer, eds.) pp. 82–91, Academic Press, New York.

HASSON, E.P. and LATIES, G.G. 1976. Separation and characterization of potato lipid acylhydrolases. Plant Physiol. *57*,142–147.

ZABORSKY, O. 1973. *Immobilized Enzymes,* pp. 28–46, CRC Press, Cleveland, Ohio.

Journal abbreviations should follow those used in *Chemical Abstracts.* Responsibility for the accuracy of citations rests entirely with the author(s). References to papers in press should indicate the name of the journal and should only be used for papers that have been accepted for publication. Submitted papers should be referred to by such terms as "unpublished observations" or "private communication." However, these last should be used only when absolutely necessary.

Tables should be numbered consecutively with Arabic numerals. The title of the table should appear as below:

Table 1. Activity of potato acyl-hydrolases on neutral lipids, galactolipids, and phospholipids

Description of experimental work or explanation of symbols should go below the table proper. Type tables neatly and correctly as tables are considered art and are not typeset. Single-space tables.

Figures should be listed in order in the text using Arabic numbers. Figure legends should be typed on a separate page. Figures and tables should be intelligible without reference to the text. Authors should indicate where the tables and figures should be placed in the text. Photographs must be supplied as glossy black and white prints. Line diagrams should be drawn with black waterproof ink on white paper or board. The lettering should be of such a size that it is easily legible after reduction. Each diagram and photograph should be clearly labeled on the reverse side with the name(s) of author(s), and title of paper. When not obvious, each photograph and diagram should be labeled on the back to show the top of the photograph or diagram.

Acknowledgments: Acknowledgments should be listed on a separate page.

Short notes will be published where the information is deemed sufficiently important to warrant rapid publication. The format for short papers may be similar to that for regular papers but more concisely written. Short notes may be of a less general nature and written principally for specialists in the particular area with which the manuscript is dealing. Manuscripts which do not meet the requirement of importance and necessity for rapid publication will, after notification of the author(s), be treated as regular papers. Regular papers may be very short.

Standard nomenclature as used in the engineering literature should be followed. Avoid laboratory jargon. If abbreviations or trade names are used, define the material or compound the first time that it is mentioned.

EDITORIAL OFFICES: DR. D.R. HELDMAN, COEDITOR, *Journal of Food Process Engineering,* National Food Processors Association, 1401 New York Avenue, N.W., Washington, D.C. 20005 USA; or DR. R.P. SINGH, COEDITOR, *Journal of Food Process Engineering,* University of California, Davis, Department of Agricultural Engineering, Davis, CA 95616 USA.

CONTENTS